Noname manuscript No.
(will be inserted by the editor)

A Spatially Disaggregated Model for the Technology Selection and Design of a Transit Line*

Luigi Moccia · Duncan W. Allen · Gilbert Laporte

the date of receipt and acceptance should be inserted later

Abstract Our research question is the usefulness of a high level of spatial granularity for the travel demand when planning a transit line. We formulate a new optimization model for the technology selection and design of a transit line where the spatial attributes of the travel demand can be finely set. The solution method relies on approximated formulae, and we establish relationships with a classic result for the optimal stop spacing. We also present a refinement of the in-vehicle passenger crowding for an existing transit design model where demand spatial attributes are set synthetically. We call "spatially disaggregate" and "spatially aggregate" the former and the latter model, respectively. These two models are compared by numerical experiments on a scenario for three semi-rapid transit technologies where two variants consider opposite demand profiles in terms of spatial distribution. We conclude that the spatially aggregated model is sufficient when the main goal is technology selection, whereas the spatially disaggregate model is better for design and benchmarking purposes.

Keywords Transit Line Design · Public Transport Optimization · Transit Technology Assessment · Semi-Rapid Transit

* This is a post-print of an article published in Public Transport (2020) 12:647–691 https://doi.org/10.1007/s12469-020-00250-0

L. Moccia
Consiglio Nazionale delle Ricerche, Istituto di Calcolo e Reti ad Alte Prestazioni, via P. Bucci, Rende, Italy
Interuniversity Research Centre on Enterprise Networks, Logistics and Transportation (CIRRELT), Canada
E-mail: moccia@icar.cnr.it

D. W. Allen
IBI Group, 21 Custom House, Boston, US 02110

G. Laporte
HEC Montréal, 3000 chemin de la Côte-Sainte-Catherine, Montréal, Canada H3T 2A7
Interuniversity Research Centre on Enterprise Networks, Logistics and Transportation (CIRRELT), Canada
School of Management, University of Bath, Claverton Down, Bath B2A 7AY, United Kingdom
E-mail: gilbert.laporte@cirrelt.net

1 Introduction

The design of a transit line and the selection of its technology are complex decisions faced by urban communities and transit operators. Quantitative assessment methods that are designed to be comprehensive can help reach a consensus among decision makers, citizens, and other stakeholders. The transit users' point of view is usually a complex topic and its modeling requires mathematical solution approaches. This paper contributes to the practical aim of broadening the scope of transit line models by considering a high spatial granularity of the travel demand and its implications on key user quality indices such as in-vehicle crowding. To this end, we present an optimization model of a transit line where spatial attributes of the passengers' boardings and alightings can be finely instantiated, and we compare this new model with another one in which these attributes are synthetically expressed. We refer to the new model as "spatially disaggregated" and to the other as "spatially aggregated". We improve the representation of the in-vehicle passenger crowding of an existing spatially aggregated model, for which we present a refinement. We compare the new spatially disaggregated and the revised spatially aggregated models on a scenario that details three technologies of two semi-rapid transit modes, namely bus rapid transit (BRT) and light rail transit (LRT). By "mode" we refer to a relatively large set of specific transit implementations that we identify as "technologies", and by "semi-rapid" we refer to the modes that require a right-of-way with partial separation from other traffic (Vuchic, 2005; Vuchic et al., 2012). The technology scenario is then divided into two variants which correspond to configurations commonly found in urban public transport systems:

- A radial case, extending between a city center or central business district and a point towards the edge of the city or in the suburbs, as depicted in Figure 1 for the light rail line in Buffalo, NY.
- A diametrical case, extending between two outlying points via the city center, as exemplified in Figure 2 for the Valley Metro Rail route in the metropolitan area of Phoenix, AZ.

The remainder of this paper is structured as follows. Section 2 reviews the relevant literature. The spatially disaggregated model and its solution method are described in Section 3. Section 4 introduces a new penalty function for the in-vehicle passenger crowding to be used in the spatially aggregated model. Numerical experiments are discussed in Section 5, and we finally draw some conclusions in Section 6.

2 Literature review

The literature stream relevant to this paper is the structural transit analysis, where examples of classic contributions are those of Vuchic and Newell (1968); Byrne (1975); Newell (1979); Wirasinghe and Ghoneim (1981). Of particular interest is the classical stop spacing formula for a non-uniform many-to-many travel demand derived by Wirasinghe and Ghoneim (1981) by means of a continuous approximation method. The modeling approach that we follow is rooted in the micro-economic appraisal of transit, a literature thread reviewed by Jara-Díaz and Gschwender (2003). The topological configuration of a transit network is a

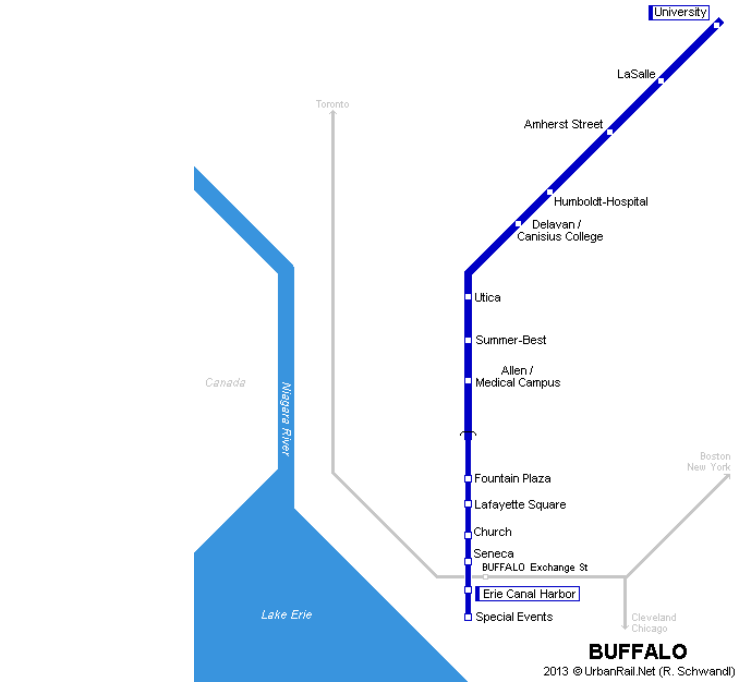

Fig. 1 Example of a radial semi-rapid rail route in Buffalo, NY. The central business district is at the route end. Source: Robert Schwandl, UrbanRail.Net.

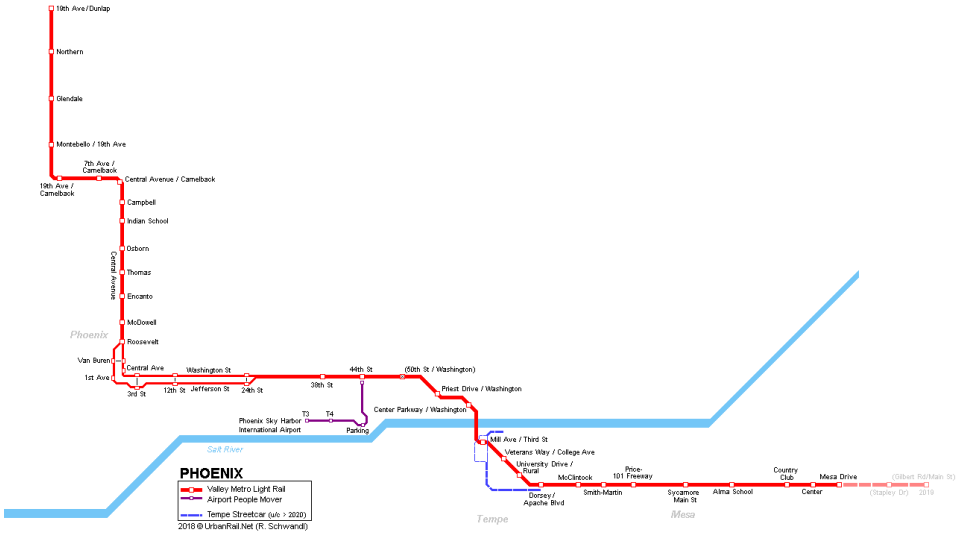

Fig. 2 Example of a diametrical semi-rapid rail route in Greater Phoenix, AZ. The portion of the route operating on Washington and Jefferson Streets is in central Phoenix. Source: Robert Schwandl, UrbanRail.Net.

wider issue which has been studied by Laporte et al. (1994, 1997) and reviewed in Gutiérrez-Jarpa et al. (2017). More generally, the research question that we pose — disaggregated versus aggregated models — has been discussed in Daganzo et al. (2012). In the following we summarize the recent research path that we extend.

Moccia and Laporte (2016) devised a lower convex approximation scheme for an optimization model of a transit line with fixed demand where the total cost, the sum of passengers and operator costs, is minimized. This approximation scheme allowed the authors to enrich the model of Tirachini et al. (2010) with variable stop spacing and train length over multiple periods while retaining some analytic treatability as in simpler models. Moreover, the approximation scheme facilitates numerical solution methods. Moccia et al. (2017) extended the model of Moccia and Laporte (2016) to a linear elastic demand and devised an equivalence scheme between the elastic and fixed demand objective functions. This scheme reinforces the equivalence in the optimality conditions proved by Daganzo (2012), and motivates a decoupling between system design and demand forecast. Thus, optimal transit configuration models can increase their level of operational detail while the demand forecast can be delegated to specialized pricing and policy setting models. Moccia et al. (2016) elaborated on techno-economic parameters of semi-rapid transit technologies with the main focus on components and design aspects yielding the best performances under realistic conditions (on this issue, see also Bruun et al. (2018)). Moccia et al. (2018) improved the model of Moccia and Laporte (2016) by new aggregate representations of the temporal and spatial variability of demand, and by refinements of the cost functions for both the operator and the passengers. This new model remains solvable by the same solution approach, the lower convex approximation scheme of Moccia and Laporte (2016), and is applied to two scenarios first outlined in Moccia et al. (2016) for two semi-rapid modes, namely BRT and LRT. We extend this research thread by devising a new optimization model where passenger demand can be spatially disaggregated. We show how the solution method of this new model can still rely on approximation formulae. The new model leds to a revised crowding penalty function of the spatially aggregated model with substantially less crowding underestimation caused by the average bias intrinsic to an aggregated model.

3 Spatially disaggregated model

This section formulates the new spatially disaggregated model and is structured as follows. We first present the notation in Section 3.1, and the principal assumptions in Section 3.2. The optimized variables are introduced in Section 3.3. The cycle time is detailed in Section 3.4. The passengers' time value and the operator cost, which are treated separately and then combined into a total cost, are described in Section 3.5 and Section 3.6, respectively. The side constraints are detailed in Section 3.7, and the resulting optimization model is presented in Section 3.8. Finally, we propose a solution method in Section 3.9. Our spatially disaggregated model shares some formulae with the spatially aggregated model of Moccia et al. (2018). To streamline the presentation, these shared formulae are omitted in this section, but we report them in Appendix A to offer a self-contained paper.

3.1 Notation

We denote as transit unit (TU), see Vuchic (2005), a set of n physically linked vehicles traveling together. For buses, n is equal to one, whereas for rail technology n can be an integer larger than one. For brevity, we denote the number of vehicles of a TU as the *TU length*. Table 1 lists the symbols that express variables. Table 2 summarizes the main symbols used as parameters, indices, and auxiliary functions. Greek letters are specific to dimensionless parameters. Additional symbols are derived as explained below. The subscripts *min* and *max* specify bounds of a parameter or of a variable. As it will be detailed in the remainder of this section, we discretize the service time in periods, the route length in sectors, and the line length in segments, indexed by p, i, and j, respectively. Parameters and variables are thus derived by using these indices as subscripts.

Table 1: List of symbols and their units of measure used as variables.

Symbol	Definition	Unit
d	Average distance between stops in a generic sector	km
$\mathbf{d}$	Vector of the stop spacings	km
f	Frequency in a generic period	TU/h
$\mathbf{f}$	Vector of $\hat{p}$ frequencies	TU/h
n	Number of vehicles per TU, also denoted as *TU length*, in a generic period	veh
$\mathbf{n}$	Vector of $\hat{p}$ TU lengths	veh

Table 2: List of primary symbols and their units of measure used as parameters, indices and auxiliary functions.

Symbol	Definition	Unit
$\bar{a}$	Average acceleration rate of a TU	m/s^2
$\bar{b}$	Average deceleration rate of a TU	m/s^2
B	Deployed fleet of TUs	TU
c_{0l}	Fixed operator cost related to the transit line	\$/h
c_{0s}	Fixed operator cost related to a stop	\$/h
c_{0sv}	Operator cost related to a stop per extra vehicle	\$/veh-h
c_{1t}	Unit operator cost per TU-hour	\$/TU-h
c_{1v}	Unit operator cost per vehicle-hour	\$/veh-h
c_{2v}	Unit operator cost per veh-km	\$/veh-km
C_a	Access and egress time value	\$/h
C_o	Operator cost	\$/h
C_u	Passengers' time value	\$/h
C_{tot}	Total cost, sum of C_u and C_o	\$/h
C_v	In-vehicle time value	\$/h
C_w	Waiting time value	\$/h
f_l	Threshold frequency for timetable behavior	TU/h
f_m	Threshold frequency for platooning	TU/h
$\dot{f}$	Threshold frequency for the high frequency penalty	TU/h
$\check{f}_{max}$	Cap on the maximum frequency	TU/h
$g_0(x)$	Index of the first segment of the direction where point x belongs	-
$g_1(x)$	Index of the segment where point x belongs	-
H	Service hours per year	h/year
i	Index of the sectors	-
j	Index of the segments	-
k	Capacity of a vehicle	pax/veh
K	Capacity of a TU	pax/TU
l	Average trip length	km
L	Length of the route	km
p	Index of the periods	-
$\hat{p}$	Number of periods	-

Continued on next page

Table 2 – *Continued from previous page*

Symbol	Definition	Unit
q	Average hourly demand at the peak period	pax/h
R	Running time in a cycle	h
s	Access and egress speed	km/h
S	Commercial speed of the TU	km/h
S_{max}	Maximum allowed speed of the TU	km/h
S_{run}	Running speed of the TU excluding stop service	km/h
t_a	Average access and egress time of a user	h
T_a	Time loss caused by acceleration and deceleration phases	h
t_b	Boarding and alighting time per user and vehicle	s/pax-veh
T_b	Boarding and alighting time per user and TU	s/pax-TU
t_{ba}	Alighting time per user and vehicle	s/pax-veh
T_{ba}	Alighting time per user and TU	s/pax-TU
t_{bb}	Boarding time per user and vehicle	s/pax-veh
T_{bb}	Boarding time per user and TU	s/pax-TU
t_c	Commercial cycle time	h
t_{oc}	Operating cycle time	h
t_d	Time loss caused by opening and closing of doors	s
t_e	Average dwell time at stops	s
$\hat{t}_e$	Maximum dwell time at stops	s
t_{e0}	Fixed stop clearance time	s
t_{ev}	Stop clearance time for an extra vehicle length	s/veh
$t_{i,j}$	TU traveling time at segment j in sector i	h
T_l	Time loss caused by acceleration, deceleration, and door operations	h
t_{tf}	Fixed component of the terminal time	s
t_{tv}	Component of the terminal time variable with the TU length	s
t_u	Average time lost at intersections per unit distance	min/km
t_v	Average in-vehicle time of a user	h
t_w	Average waiting time of a user	h
$u_1(i)$	Segment index in the first direction of sector i	-
$u_2(i)$	Segment index in the second direction of sector i	-
V_a	Unit value of the access and egress time	\$/pax-h
V_v	Unit value of the in-vehicle time	\$/pax-h
V_w	Unit value of the waiting time	\$/pax-h
w	Waiting time at a stop when $f < f_l$	min
x	One-dimension coordinate of a point of the transit line	km
y	One-stage technical life	year
α	Fraction of the hourly demand in the most loaded segment of the line	-
β	Multiplicative factor of the operating cycle time	-
γ	Ratio of the period demand to the peak demand	-
δ	Crowding penalty function wrt the instantaneous occupancy rate	-
Δ, Δ_2	Crowding penalty functions wrt the average occupancy rate	-
ϵ	Rate of the average waiting time to the headway	-
ζ	Spare capacity factor for the fleet	-
η	Fraction of the longest dwell time in the maximum frequency formula	-
θ	Vehicle occupancy rate	-
ι	Discount rate	-
λ	Ratio of the average trip length to the length of the route	-
Λ_i	Ratio of sector i length to the route length	-
μ	Discount factor of the waiting time under timetable behavior	-
ν	Spare capacity factor for the TU	-
ξ	Parameter of the crowding penalty function δ	-
Ξ	Ratio of the residual value to the initial value of a capital component	-
π_j	Fraction of the boardings at segment j	-
ρ	Slope of the linear part of the crowding penalty function δ	-
σ_j	Fraction of the alightings at segment j	-
τ	Ratio of the maximum to the average period demand	-
$\upsilon(x)$	Ratio of the sub-segment induced by x to $g_1(x)$	-
$\Upsilon(x)$	Cumulative difference between fractional boardings and alightings at x	-
$\bar{\Upsilon}_j$	Cumulative difference between fractional boardings and alightings at the mid-segment j	-
ϕ	Ratio of the maximum to the average vehicle occupancy rate	-
ψ	Ratio of the maximum to the average dwell time	-
χ	Ratio of the period hours to the total service hours	-
$\omega_{(1,2)}$	Parameters of the high frequency penalty	-

3.2 Main assumptions

We assume that a bidirectional transit line operates on a route, where by "route" we designate the physical alignment and the infrastructure, and by "line" we refer to the service operated. We present the model for a route that connects two termini with zero passenger flow between the two directions, i.e. the route is not a loop. This is the most common case and it simplifies the notation.

The route length is L, and the line length between the termini is $2L$. The route is partitioned into m sectors, and a sector i, $i \in \{1, ..., m\}$, has length $\Lambda_i L$, where the Λ_i parameters are positive real numbers with $\sum_i \Lambda_i = 1$. The route partition into m sectors induces a line partition into $2m$ segments. One direction of the line, called the first direction, consists of segments indexed by $j \in \{1, ..., m\}$, and the other direction, called the second direction, is composed of segments indexed by $j \in \{m+1, ..., 2m\}$. Two functions $u_1(i)$ and $u_2(i)$ return the segments' indices of the first and second direction in sector i, respectively. Function $e(j)$ returns the sector index of segment j. Thus, a sector i consists of two segments with indices $u_1(i) = i$ and $u_2(i) = 2m + 1 - i$, and $e(i) = e(2m + 1 - i) = i$. Figure 3 illustrates these definitions.

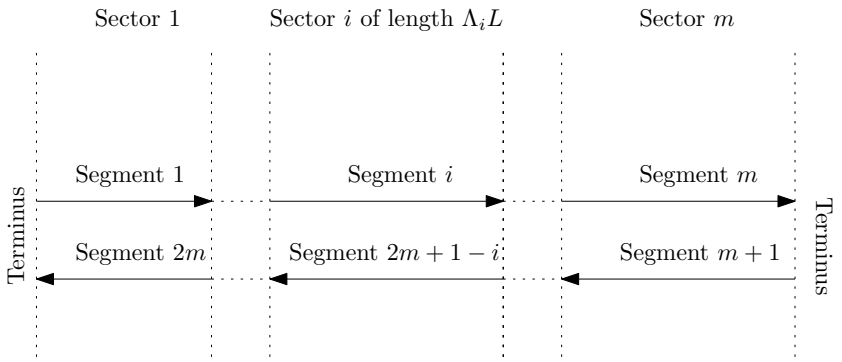

Fig. 3 Route sectors and line segments.

The transit line serves passengers for $\hat{p}$ periods in the operation year. The average bidirectional hourly demand q_p in period p is equal to $q\gamma_p$, where p is the period index in the set $\{1, ..., \hat{p}\}$, γ_p is a positive parameter not larger than one, and q is the average hourly demand during the peak period. The average hourly demand in a period indicates that q_p boardings and q_p alightings per hour occur on average along the line in that period. We index the periods in non-increasing order of demand, the peak period is indicated by $p = 1$ and hence $\gamma_1 = 1$. The maximum demand per period is $q_p\tau_p$, where $\tau_p > 1$. The ratio of a period's hours to the total service hours is denoted by χ_p, and $\sum_p \chi_p = 1$. These demand parameters must reflect the total service hours in a year, indicated by H.

In a sector the boardings and alightings per segment and per period can be assumed as uniform values as explained in the following. We indicate by $\pi_{j,p}$ and $\sigma_{j,p}$ the fractions of the average boardings and alightings, respectively, in period p at segment j, with $j \in \{1, ..., 2m\}$. Uniform values for boarding and alighting in a sector i mean that in each period these passenger activities are requested

along the sector's segments with the densities $\pi_{u_1(i),p}/\Lambda_i$, $\sigma_{u_1(i),p}/\Lambda_i$, $\pi_{u_2(i),p}/\Lambda_i$, and $\sigma_{u_2(i),p}/\Lambda_i$. For notational simplicity, when we refer to a generic period we omit the period index. By definition, the fractions of the average boardings and alightings are such that $\sum_j \pi_j = \sum_j \sigma_j = 1$. The assumption of zero passenger flow between the two directions implies a boarding and alighting balance for each direction:

$$\begin{aligned} \sum_{j=1}^{m} \pi_j &= \sum_{j=1}^{m} \sigma_j \\ \sum_{j=m+1}^{2m} \pi_j &= \sum_{j=m+1}^{2m} \sigma_j. \end{aligned} \tag{1}$$

The total fractional passenger activity at a sector, indicated by Θ_i, is the sum of the fractional boardings and aligthings at the pertaining segments:

$$\Theta_i = \pi_{u_1(i)} + \sigma_{u_1(i)} + \pi_{u_2(i)} + \sigma_{u_2(i)}. \tag{2}$$

A point along the line is indicated by a one-dimensional coordinate x, with $0 \leq x \leq 2L$. Let $g_0(x)$ and $g_1(x)$ be the indices of the first segment of the direction and of the segment where the point x belongs, respectively. We denote by $\upsilon(x)$ the ratio between the length of the sub-segment starting at the extremum of segment $g_1(x)$ closer to $g_0(x)$ and ending at x, and that of the segment $g_1(x)$. Thus, the coordinate x can be expressed as

$$x = L \left(\max\{g_0(x) - m, 0\} + \sum_{j=g_0(x)}^{g_1(x)-1} \Lambda_{e(j)} + \Lambda_{e(g_1(x))} \upsilon(x) \right). \tag{3}$$

The difference between the cumulative fractional boardings and alightings in period p and at the point x along the line is indicated by $\Upsilon_p(x)$, and for a generic period:

$$\Upsilon(x) = \sum_{j=g_0(x)}^{g_1(x)-1} (\pi_j - \sigma_j) + \left(\pi_{g_1(x)} - \sigma_{g_1(x)}\right) \upsilon(x). \tag{4}$$

By construction, $\Upsilon(x)$ is continuous and piecewise linear, hence its extrema occur at some segment boundaries. The $\Upsilon(x)$ value occurring at the midpoint in a segment j, i.e. $g_1(x) = j$ and $\upsilon(x) = 0.5$, is denoted by $\bar{\Upsilon}_j$. The maximum $\bar{\Upsilon}$ value is denoted by α, and a segment where it occurs is defined as "most loaded segment" (MLS). Figure 4 illustrates an example of these values.

3.3 Variables

The average stop spacing in a sector i is an optimized continuous variable and is denoted by d_i. We denote by n_p the number of vehicles of a TU in period p, and this an integer variable that we optimize. The frequency f is expressed as the number of TUs per hour. There is a frequency for each period, namely f_p, and this is also a continuous variable that is optimized.

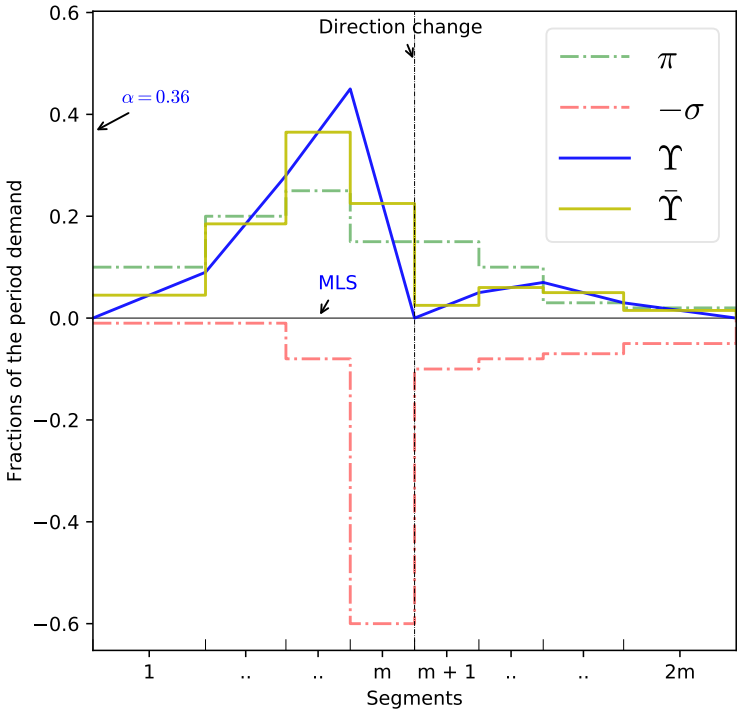

Fig. 4 An example of boardings and alightings in a transit line with $m = 4$. Segment's fractional boardings, π, and negative alightings, $-\sigma$, are depicted as dash-and-dot step functions. The cumulative difference between fractional boardings and alightings, Υ, is the solid piecewise linear function with zero value at the termini coordinates, and its mid-segment values, $\bar{\Upsilon}$, is the solid step function.

3.4 Cycle time

We distinguish between operating and commercial cycle times. The *operating cycle time* is the sum of the running time between stations, including acceleration and deceleration, of the time lost at intersections, and of the dwell time for boarding and alighting. The *commercial cycle time* is determined as a function of the operating cycle time to include operations at terminals and the provision for running time variability.

More formally, we model the operating cycle time as the sum of four terms described in the following. We assume that a TU accelerates up to and decelerates from a speed S_{max} which is the maximum allowable speed. The TU loses an average t_u minutes per km. This time loss occurs mainly at intersections and diminishes with higher investments in runningway improvements and traffic signal priority (TSP) systems. This phenomenon induces an average speed excluding user service at stops, S_{run}, less than S_{max}, and computed by formula (38) in

Appendix A. The resulting running time, denoted R, is equal to $2L/S_{run}$ and is the first term of the operating cycle time. We assume that on average a TU leaves a stop accelerating up to S_{run}, travels at this speed, and then decelerates to halt at the next stop. Given the average acceleration and deceleration rates of a TU, the incremental time loss caused by the acceleration and deceleration phases, T_a, is computed by (39). We add to the standing time a fixed component t_d, which accounts for the opening and closing of the doors, and we denote by T_l the lost time for acceleration, deceleration, and door opening and closing, see formula (40). Because the number of stops is equal to $2L\sum_i \Lambda_i/d_i$, the second term of the operating cycle time is $2LT_l\sum_i \Lambda_i/d_i$. The third term of the operating cycle time expresses the load-dependent dwell time which is related to T_b, the boarding and alighting time per user of a TU, and the number of passengers boarding and alighting a TU, given by q/f. The parameter T_b is sum of two components, T_{bb} and T_{ba}, related to the boarding and the alighting activities, respectively. The boarding and alighting time of a TU depends on the number n of vehicles per TU and their door configuration. We assume the boarding and alighting service times per user of a vehicle to be equal to t_{bb} and t_{ba}, respectively, hence $T_{bb} = t_{bn}/n$ and $T_{ba} = t_{ba}/n$. We introduce a fourth term of the operating cycle time accounting for extra delays at intersections, links, and stops under high frequencies, where for high frequencies we mean those exceeding a threshold frequency $\dot{f}$, for example 25 TU/h. When this frequency is reached, the design TSP may underperform, and the interactions between signals and stops, as well as the disturbances induced by trespassing, may become significant. This term depends on the ratio of the frequency to this threshold frequency raised to the power ω_2, and multiplied by a coefficient ω_1 to the base operating cycle time loss at intersections, which is equal to $2t_uL$ (Moccia et al., 2018). The operating cycle time $t_{oc,p}$ for each period is

$$t_{oc,p}(f_p, \mathbf{d}, n_p) = R + 2LT_l \sum_i \frac{\Lambda_i}{d_i} + \frac{t_{bb} + t_{ba}}{3600}\frac{q_p}{n_p f_p} + \omega_1 \frac{2t_u L}{60}\left(\frac{f_p}{\dot{f}}\right)^{\omega_2}$$
$$t_{bb}, t_{ba}[\text{s-pax/veh}], q_p[\text{pax/h}], T_l, R[\text{h}], t_u[\text{min/km}], d_i, L[\text{km}],$$
$$n_p[\text{veh/TU}], f_p, \dot{f}[\text{TU/h}], \quad (5)$$

where $\mathbf{d}$ is the vector of m stop spacings.

The commercial cycle time is obtained by multiplying the operating cycle time by β, a parameter larger than one that accounts for the schedule time recovery at the terminals, and by adding the following two terms. First, a fixed terminal time t_{tf} that accounts for minimum crew rest, securing vehicle keys, and in some cases navigating a terminal loop. Second, a terminal time proportional to t_{tv} and variable with the TU length that accounts for the crew walking distance between the TU ends, and safety checks. The commercial cycle time, hereinafter referred to as cycle time for brevity, is

$$t_{c,p}(f_p, \mathbf{d}, n_p) = \beta t_{oc,p}(f_p, \mathbf{d}, n_p) + \frac{t_{tf} + t_{tv} n_p}{3600}$$
$$t_{oc,p}[\text{h}], n_p[\text{veh/TU}], t_{tf}[\text{s}], t_{tv}[\text{s/veh}]. \quad (6)$$

3.5 Passengers' time value

The passenger time value is a monetized value of time composed of three parts: access and egress, waiting, and in-vehicle time values.

Users access and egress the nearest stop at speed s. The average distance is $d_i/4$ for an access or an egress at segment i, and the average access and egress time $t_{a,i}$ of a user is

$$t_{a,i} = \frac{d_i}{4s} \quad d[\text{km}], s[\text{km/h}]. \tag{7}$$

The value of one unit of access and egress time is expressed by the parameter V_a, and the average access and egress value C_a for the line is

$$C_a(\mathbf{d}) = V_a q \sum_i \sum_p \Theta_{i,p} \frac{d_i}{4s} \gamma_p \chi_p. \tag{8}$$

The waiting time depends on the frequency and we distinguish among low, medium and high frequencies. In the case of high frequencies, defined as those above a threshold frequency f_m, users arrive at stops at a constant rate but TU platooning[1] starts to occur. Because of platooning, the additional TU capacity provided by frequencies larger than f_m do not yield a further reduction in the average headway with respect to $1/f_m$. Thus, the average waiting time t_w can be modeled as a fraction $\epsilon \geq 1/2$ of the expected headway. Values of ϵ strictly larger than $1/2$ can model cases where the headways have a large variance. In the case of medium frequencies, users arrive at stops at a constant rate and the average waiting time is ϵ/f. In the case of low frequencies, users follow timetables and arrive at stops w minutes before the expected time of service. The waiting time at the stop saved by this behavior still represents a disutility for the user who may have to redefine his schedule. This disutility, often referred to as schedule delay, is discounted by a factor μ less than one, for example $\mu = 1/3$, with respect to the disutility of waiting at the stop. The threshold frequency for these two former behavior regimes is defined by f_l, for example six TU per hour, which results in a headway of 10 minutes. The average waiting time t_w of a user is computed by formula (41). The average value of waiting $c_w(f)$ borne by q users at the frequency f is

$$c_w(f) = V_w t_w(f) q \quad V_w[\$/\text{pax-h}], t_w[\text{h}], q[\text{pax/h}], \tag{9}$$

where V_w is the value of one waiting time unit. The average value of waiting for the $\hat{p}$ periods, C_w, is

$$C_w(\mathbf{f}) = \sum_p c_w(f_p) \gamma_p \chi_p \quad c_w[\$/\text{h}], \tag{10}$$

where $\mathbf{f}$ is the vector of $\hat{p}$ frequencies.

The in-vehicle time of passengers is modeled as the product of the traveling time of a TU in a segment and the average passenger flow in that segment. Similarly

[1] We use the term "platooning" to indicate the unorganized formation of clumps of vehicles. This occurrence may also be referred to as "bunching".

to the operating cycle time, $t_{oc,p}$, we define the traveling time of a TU in a segment j belonging to a sector i, in a period p, $t_{i,j,p}$, as

$$t_{i,j,p}(f_p, d_i, n_p) = R\frac{\Lambda_i}{2} + T_l\frac{\Lambda_i L}{d_i} + \frac{t_{bb}\pi_{j,p} + t_{ba}\sigma_{j,p}}{3600}\frac{q_p}{n_p f_p} + \omega_1\frac{t_u \Lambda_i L}{60}\left(\frac{f_p}{\dot{f}}\right)^{\omega_2}$$
$$t_{bb}, t_{ba}[\text{s-pax/veh}], q_p[\text{pax/h}], T_l, R[\text{h}], t_u[\text{min/km}], d_i, L[\text{km}],$$
$$n_p[\text{veh/TU}], f_p, \dot{f}[\text{TU/h}] \quad (11)$$

The value of the in-vehicle travel time is multiplied by a crowding penalty function δ, which depends on the average occupancy rate $\bar{\theta}_{j,p}$ on segment j in period p. The average occupancy rate depends on the frequency and on the TU length:

$$\bar{\theta}_{j,p}(f_p, n_p) = \frac{\bar{\Upsilon}_{j,p} q_p}{k n_p f_p}, \quad (12)$$

where k is the passenger capacity of a vehicle, and hence the capacity K of a multi-unit TU is equal to $k \times n$. The function δ is piecewise linear as follows: there is no penalty up to an average occupancy rate of θ_{min}, e.g. it is equal to 0.3, and for larger values the penalty increases linearly with a slope value ρ. Figure 5 provides an example of this penalty function. Moccia et al. (2017, 2018) discuss the relevant literature that supports this approach for in-vehicle passenger crowding.

Formally, the penalty function is

$$\delta_{j,p}(f_p, n_p) = \begin{cases} 1 + \rho\left(\bar{\theta}_{j,p} - \theta_{min}\right) = \xi + \rho\dfrac{\bar{\Upsilon}_{j,p} q_p}{k n_p f_p} & n_p f_p \leq \dfrac{\bar{\Upsilon}_{j,p} q_p}{k\theta_{min}} \\ 1 & \text{otherwise} \end{cases}, \quad (13)$$

where $\xi = 1 - \theta_{min}\rho$ is a parameter introduced for notational compactness.

Let V_v be the value of one unit of in-vehicle time, then the value of in-vehicle time, C_v, is

$$C_v(\mathbf{f}, \mathbf{d}, \mathbf{n}) = V_v q \sum_p \sum_j \chi_p \gamma_p \bar{\Upsilon}_{j,p} \delta_{j,p}(f_p, n_p) t_{e(j),j,p}(f_p, d_{e(j)}, n_p), \quad (14)$$

where $\mathbf{n}$ is the vector of $\hat{p}$ TU lengths. The total passengers' time value C_u is then

$$C_u = C_a + C_w + C_v \quad C_a, C_w, C_v[\$/\text{h}]. \quad (15)$$

3.6 Operator cost

The operator cost consists of six components. The first is the construction and maintenance of the route and is denoted by c_{0l}. The second and third components are related to the construction and maintenance costs of the stations. For each station these costs can be decomposed into a fixed part c_{0s}, and a variable part c_{0sv}, which depends on the TU length at peak hours. There are $2 + 2L\sum_i \Lambda_i/d_i$ one-way stops, including the terminal. The second component is related to the terminal, and the third to the other stops which depends on the stop spacings. The fourth component depends on the fleet size and reflects vehicle capital and administrative costs. Let c_{1v} be the unit operator cost per vehicle-hour which

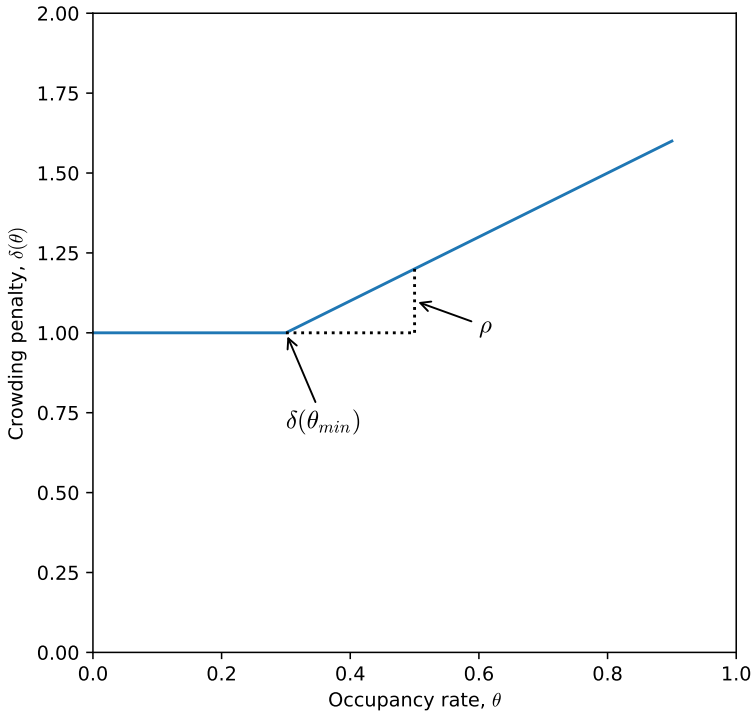

Fig. 5 Example of the crowding penalty function with $\rho = 1$ and $\theta_{min} = 0.3$.

accounts for the capital and administrative costs. The deployed fleet size B of TUs is the product of frequency and cycle time: $B = ft_c$. The vehicle fleet size is equal to ζnB, where $\zeta > 1$ provides for O&M spares. The fifth component expresses the crew costs and depends on c_{1t}, the unit operator cost per TU-hour. The sixth component accounts for running costs such as energy, tires, lubricants, etc. Let c_{2v} be the unit operator cost per vehicle-km. The amount of vehicle-km is the product of the commercial speed S and the fleet size. The commercial speed is obtained by dividing the total length $2L$ by the cycle time. Thus, the amount of vehicle-km is $S \times nB = 2L/t_c \times nft_c = 2Lnf$.

The operator cost C_o is then

$$\begin{aligned} C_o(\mathbf{f},\mathbf{d},\mathbf{n}) = {} & c_{0l} + 2(c_{0s} + c_{0sv}(n_1 - 1)) + 2L(c_{0s} + c_{0sv}(n_1 - 1)) \sum_i \frac{\Lambda_i}{d_i} \\ & + c_{1v}\zeta n_1 f_1 t_{c,1}(f_1, \mathbf{d}, n_1) + c_{1t} \sum_p \chi_p f_p t_{c,p}(f_p, \mathbf{d}, n_p) \\ & + 2c_{2v} L \sum_p \chi_p n_p f_p. \end{aligned} \tag{16}$$

We note that this formula is different from that of the spatially aggregated model of Moccia et al. (2018) because the second component was not considered in that model. In the following, when we compare results with the spatially aggregated model we consider a revised version of the spatially aggregated model which includes this cost component.

3.7 Side constraints

The frequency is constrained to be equal to or larger than f_{min}, and less than or equal to f_{max}. The value f_{min} can be set by a "policy headway" rationale, i.e. there is a minimum guaranteed frequency f_{pol}, or can account for capacity as follows. Recall that α is the maximum difference between the cumulative fractional boardings and alightings along the line. Henceforth, $\alpha q \tau$ is the largest load served by the line in a generic period. Let ν be a spare capacity design factor. For example, a value of ν smaller than one accounts for random demand fluctuations and represents a safety margin, whereas ν larger than one allows some occurrence of crush loading. The lower bound for the frequency is defined in (42). The f_{max} is defined according to general principles from the Transit Capacity and Quality of Service Manual (TCQSM, 2013). We set a cap $\check{f}_{max}$ on the value of f_{max} to reflect a rail vehicle operation with drivers responsible for maintaining safe separation. For buses $\check{f}_{max}$ can attain a larger value, around the double of that for rail. For BRT and LRT operations within or parallel to urban arterial roadways the minimum achievable headway depends on the longest dwell time. The longest dwell time, $\hat{t}_e$, is a function of frequency, stop spacings, and TU length:

$$\hat{t}_e(f, \mathbf{d}, n) = t_d + \frac{q}{nf} \max_j \frac{(t_{bb}\pi_j + t_{ba}\sigma_j) d_{e(j)}}{L \Lambda_{e(j)}} \quad \begin{array}{l} t_{ba}, t_{bb}[\text{s-pax/veh}], q[\text{pax/h}], \\ d_{e(j)}, L[\text{km}], n[\text{veh/TU}], \\ f[\text{TU/h}]. \end{array} \tag{17}$$

The f_{max} formula for the bus and light rail modes share the following common form:

$$f_{max}(f, \mathbf{d}, n) = \min \left\{ \check{f}_{max}, \frac{3600}{t_{e0} + t_{ev}(n-1) + \eta \hat{t}_e} \right\} \quad \begin{array}{l} \check{f}_{max}[\text{TU/h}], \\ t_{e0}, t_{ev}, \hat{t}_e[\text{s}], \end{array} \tag{18}$$

where t_{e0} is the fixed stop clearance time, t_{ev} is the stop clearance time for an extra vehicle length, and η is a fraction of the longest dwell time.

Finally, we impose side constraints on the average stop spacing. Reaching the speed S_{max} requires a stop spacing larger than a threshold value d_{min}, which depends on acceleration and deceleration rates according to formula (43). An upper bound d_{max} is also defined.

3.8 Optimization model

The total cost C_{tot}, sum of passengers' time value and operator cost, is a function of frequencies, stop spacings, and TU lengths. The model follows:

$$\text{minimize } C_{tot}(\mathbf{f}, \mathbf{d}, \mathbf{n}) \tag{19}$$

subject to

$$d_{min} \leq d_i \leq d_{max}, \forall i \in \{1, ..., m\} \tag{20}$$

$$\max\left\{f_{pol,p}, \frac{\alpha_p q_p \tau_p}{\nu n_p k}\right\} \leq f_p \leq f_{max,p}(f_p, \mathbf{d}, n_p), \forall p \in \{1, ..., \hat{p}\} \tag{21}$$

$$n_{min} \leq n_p \leq n_{max},\ n_p \in \mathbb{N}, \forall p \in \{1, ..., \hat{p}\} \tag{22}$$

$$n_p f_p t_{c,p}(f_p, d, n_p) \leq n_1 f_1 t_{c,1}(f_1, d, n_1), \forall p \in \{2, ..., \hat{p}\}. \tag{23}$$

Constraints (20) set minimum and maximum values for the stop spacings. Constraints (21) enforce minimum and maximum values for the frequencies. Constraints (22) specify the feasible range of TU lengths, and constraint (23) ensures that the maximum fleet is deployed at peak times, where for "maximum deployed fleet" we refer to the number of vehicles needed for the scheduled service (the reserve that bears a capital cost is accounted in the operator cost function).

3.9 Solution method

The model is solved by an updated version of the algorithm presented in Moccia and Laporte (2016). We construct a separable lower convex envelope of the objective function C_{tot} in the feasible frequency range as follows. First, we use the lower linear value of the crowding penalty. Second, we assume a discounted waiting time by the factor μ whenever the minimum frequency is smaller than f_l. Third, we compute the intersection delay in the cycle time at the minimum frequency. Fourth, we remove non-convex terms by fixing some variables to proper bounds.

Thus, we can define a separable lower convex envelope of the objective function for a given vector of TU lengths $\bar{\mathbf{n}}$ as

$$\begin{aligned}
&\tilde{C}_{tot}(\mathbf{f}, \mathbf{d}, \bar{\mathbf{n}}) = \frac{V_a q}{4s} \sum_i d_i \sum_p \Theta_{i,p} \gamma_p \chi_p + V_w q \sum_p \gamma_p \chi_p \mu_p \frac{\epsilon}{f_p} + \\
&V_v q \sum_p \sum_j \chi_p \gamma_p \bar{\Upsilon}_{j,p} \left[\xi \left(\frac{R\Lambda_{e(j)}}{2} + \frac{t_{bb}\pi_{j,p} + t_{ba}\sigma_{j,p}}{3600 \bar{n}_p f_p} q_p + \omega_1 \frac{t_u \Lambda_{e(j)} L}{60} \left(\frac{f_{min,p}}{\dot{f}}\right)^{\omega_2}\right) + \right. \\
&\left(\rho \frac{\bar{\Upsilon}_{j,p} q_p}{k \bar{n}_p f_p}\right) \left(\frac{R\Lambda_{e(j)}}{2} + \frac{t_{bb}\pi_{j,p} + t_{ba}\sigma_{j,p}}{3600 \bar{n}_p f_{max,p}} q_p + \omega_1 \frac{t_u \Lambda_{e(j)} L}{60} \left(\frac{f_{min,p}}{\dot{f}}\right)^{\omega_2}\right) + \\
&\left.\left(\xi + \rho \frac{\bar{\Upsilon}_{j,p} q_p}{k \bar{n}_p f_{max,p}}\right) \frac{T_l \Lambda_{e(j)} L}{d_{e(j)}}\right] + \\
&c_{0l} + 2(c_{0s} + c_{0sv}(\bar{n}_1 - 1)) + 2L(c_{0s} + c_{0sv}(\bar{n}_1 - 1)) \sum_i \frac{\Lambda_i}{d_i} + \\
&c_{1v} \zeta \bar{n}_1 f_1 \left(\beta \left(R + \frac{2LT_l}{d_{max}} + \frac{t_{bb} + t_{ba}}{3600} \frac{q}{\bar{n}_1 f_1} + \omega_1 \frac{2t_u L}{60} \left(\frac{f_{min,1}}{\dot{f}}\right)^{\omega_2}\right) + \frac{t_{tf} + t_{tv} \bar{n}_1}{3600}\right) + \\
&c_{1t} \sum_p \chi_p f_p \left(\beta \left(R + \frac{2LT_l}{d_{max}} + \frac{t_{bb} + t_{ba}}{3600} \frac{q_p}{\bar{n}_p f_p} + \omega_1 \frac{2t_u L}{60} \left(\frac{f_{min,p}}{\dot{f}}\right)^{\omega_2}\right) + \frac{t_{tf} + t_{tv} \bar{n}_p}{3600}\right) + \\
&2c_{2v} L \sum_p \chi_p \bar{n}_p f_p = \\
&= a_0 + \sum_i a_{1,i} d_i + \sum_i \frac{a_{2,i}}{d_i} + \sum_p a_{3,p} f_p + \sum_p \frac{a_{4,p}}{f_p},
\end{aligned} \tag{24}$$

where the coefficients of the previous equation are defined as

$$
\begin{aligned}
a_0 &= c_{0l} + 2(c_{0s} + c_{0sv}(\bar{n}_1 - 1)) + c_{1v}\zeta\beta q\frac{t_{bb}+t_{ba}}{3600} + c_{1t}\beta q\frac{t_{bb}+t_{ba}}{3600}\sum_p \frac{\chi_p\gamma_p}{\bar{n}_p} + \\
&\quad V_v q\xi\sum_p\sum_j \chi_p\gamma_p\bar{\Upsilon}_{j,p}\frac{\Lambda_{e(j)}}{2}\left(R + t_{\omega,p}\right) \\
a_{1,i} &= \frac{V_a q}{4s}\sum_p \Theta_{i,p}\gamma_p\chi_p \\
a_{2,i} &= 2L\Lambda_i(c_{0s} + c_{0sv}(\bar{n}_1 - 1)) + \\
&\quad 2L\Lambda_i T_l V_v q\sum_p \chi_p\gamma_p\left(\bar{\Upsilon}_{u_1(i),p}\left(\xi + \rho\frac{\bar{\Upsilon}_{u_1(i),p}q_p}{k\bar{n}_p f_{max,p}}\right) + \bar{\Upsilon}_{u_2(i),p}\left(\xi + \rho\frac{\bar{\Upsilon}_{u_2(i),p}q_p}{k\bar{n}_p f_{max,p}}\right)\right) \\
a_{3,p} &= 2c_{2v}L\chi_p\bar{n}_p + {}_{\text{if } p=1}\, c_{1v}\zeta\bar{n}_1\left(\beta\left(\frac{2LT_l}{d_{max}} + t_{\omega,1}\right) + R_1^{'}\right) + \\
&\quad c_{1t}\chi_p\left(\beta\left(\frac{2LT_l}{d_{max}} + t_{\omega,p}\right) + R_p^{'}\right) \\
a_{4,p} &= V_w q\epsilon\gamma_p\chi_p\mu_p + V_v q\sum_j \chi_p\gamma_p\bar{\Upsilon}_{j,p}\left[\xi\frac{t_{bb}\pi_{j,p} + t_{ba}\sigma_{j,p}}{3600\bar{n}_p}q_p + \right. \\
&\quad \left.\left(\rho\frac{\bar{\Upsilon}_{j,p}q_p}{k\bar{n}_p}\right)\left(\frac{t_{bb}\pi_{j,p} + t_{ba}\sigma_{j,p}}{3600\bar{n}_p f_{max,p}}q_p + \frac{\Lambda_{e(j)}}{2}(R + t_{\omega,p})\right)\right],
\end{aligned}
\tag{25}
$$

and where, for notational compactness, we have used the following notation:

$$
\begin{aligned}
R_p^{'} &= \beta R + \frac{t_{tf} + t_{tv}\bar{n}_p}{3600} \\
\mu_p &= \begin{cases} \mu & \text{if } \; f_{min,p} < f_l \\ 1 & \text{if } \; f_{min,p} \geq f_l \end{cases} \\
t_{\omega,p} &= \omega_1\frac{2t_u L}{60}\left(\frac{f_{min,p}}{\dot{f}}\right)^{\omega_2}.
\end{aligned}
\tag{26}
$$

By calculus, the unconstrained optimal stop spacings, $\tilde{d}_{unc,i}$, and frequencies, $\tilde{f}_{unc,p}$, of the approximation are

$$
\tilde{d}_{unc,i} = \sqrt{\frac{a_{2,i}}{a_{1,i}}} \tag{27}
$$

$$
\tilde{f}_{unc,p} = \sqrt{\frac{a_{4,p}}{a_{3,p}}}. \tag{28}
$$

Table 3 reports these formulae.

We now comment on similarities and differences between our approximated stop spacing formula and that of Wirasinghe and Ghoneim (1981) (equation (10), page 215). Both formulae are twice the square root of a ratio with two components at the numerator and a denominator that expresses the product of the access value of time and the combined demand for boarding and alighting per unit of length. In both formulae, the two components at the denominator relate to the extra-costs of a stop for the operator and the on-board passengers. These extra-costs differ

between the two formulae as follows. The operator extra-cost in our formula is only related to the construction and maintenance of a stop whereas that of Wirasinghe and Ghoneim (1981) is also related to the effect of the stop time loss on fleet costs. This effect is included in our model, but because of the approximation scheme based on some variable fixing, it does not appear in the stop spacing formula. The extra-cost for on-board passengers in our formula includes a quadratic term in the average occupancy because of the in-vehicle crowding. This effect was not considered in the model of Wirasinghe and Ghoneim (1981). We further observe that Vuchic and Newell (1968) in their review of passenger transportation studies performed between 1915 and 1930 highlighted that these early works were the first to point that an optimal stop spacing should be a function of the number of on-board passengers and of those wishing to board it.

4 In-vehicle passenger crowding for the spatially aggregated model

In-vehicle passenger crowding is underestimated when the vehicle occupancy rate varies along the cycle time and an average vehicle occupancy is used to synthetically gauge crowding. In the following we denote by t the time step belonging to the cycle time, and we consider for notational brevity a cycle time of unitary length, i.e. $t \in [0, 1]$. The crowding penalty function δ is that of equation (13) and it is piecewise linear and convex. Let $\theta(t)$ be the instantaneous vehicle occupancy rate, then, because of the convexity of δ, we have the following Jensen inequality (Jensen, 1906):

$$\delta(\bar{\theta}) = \delta\left(\int_0^1 \theta(t)\mathrm{d}t\right) \leq \int_0^1 \delta(\theta(t))\mathrm{d}t. \tag{29}$$

Moccia et al. (2018) introduce a function Δ that corrects the underestimation caused by Jensen's inequality when the occupancy rate can be approximated by a linear function. Here, we present a further refinement by a new function Δ_2 such that, under the same assumption of linear approximation of the occupancy rate, the following holds:

$$\bar{\theta}\Delta_2(\bar{\theta}) = \textstyle\int_0^1 \theta(t)\delta(\theta(t))\mathrm{d}t. \tag{30}$$

Observe that the integration in the right-hand side of the previous equation is equivalent to the summation performed in our spatially disaggregated model, and the left-hand side is the equivalent term in the aggregated model of Moccia et al. (2018). Henceforth, this new function Δ_2 would replace the function Δ in the model of Moccia et al. (2018).

As in Moccia et al. (2018), and without loss of generality, we use a non-increasing function $\theta(t)$, i.e. the occupancy rate is ordered in the time index such that the maximum occurs at $t = 0$ and its equal to $\phi\bar{\theta}$, where ϕ is a parameter larger than or equal to one. The smaller abscissa such that $\theta(t) = 0$ is indicated by b, and if this does not occur b is set to one. The users' time in the unitary cycle time is an invariant, i.e. $\int_0^1 \theta(t)\mathrm{d}t = \bar{\theta}$. Henceforth, under the above assumptions, given $\bar{\theta}$ and ϕ we can uniquely determine the parameters of this function that has the following general form

$$\theta(t) = \begin{cases} \phi\bar{\theta} - ct & t \in [0, b] \\ 0 & t \in (b, 1], \end{cases} \tag{31}$$

Table 3 Formulae of the unconstrained optimal stop spacings and frequencies of the approximation.

$$\tilde{d}_{unc,i} = 2\sqrt{\frac{2sL\Lambda_i\left[(c_{0s}+c_{0sv}(\bar{n}_1-1))+T_lV_vq\sum_p\chi_p\gamma_p\left(\bar{\Upsilon}_{u_1(i),p}\left(\xi+\rho\frac{\bar{\Upsilon}_{u_1(i),p}q_p}{k\bar{n}_pf_{max,p}}\right)+\bar{\Upsilon}_{u_2(i),p}\left(\xi+\rho\frac{\bar{\Upsilon}_{u_2(i),p}q_p}{k\bar{n}_pf_{max,p}}\right)\right)\right]}{V_aq\sum_p\Theta_{i,p}\gamma_p\chi_p}}.$$

$$\tilde{f}_{unc,p} = \sqrt{q\gamma_p\frac{V_w\epsilon\mu_p+V_v\sum_j\bar{\Upsilon}_{j,p}\left[\xi\frac{t_{bb}\pi_{j,p}+t_{ba}\sigma_{j,p}}{3600\bar{n}_p}q_p+\left(\rho\frac{\bar{\Upsilon}_{j,p}q_p}{k\bar{n}_p}\right)\left(\frac{t_{bb}\pi_{j,p}+t_{ba}\sigma_{j,p}}{3600\bar{n}_pf_{max,p}}q_p+\frac{\Lambda_{e(j)}}{2}(R+t_{\omega,p})\right)\right]}{2c_{2v}L\bar{n}_p+_{\text{if }p=1}\frac{c_{1v}\zeta\bar{n}_1}{\chi_1}\left(\beta\left(\frac{2LT_l}{d_{max}}+t_{\omega,1}\right)+R_1'\right)+c_{1t}\left(\beta\left(\frac{2LT_l}{d_{max}}+t_{\omega,p}\right)+R_p'\right)}}.$$

where c is the negative of the slope. A value of ϕ not larger than two causes b equal to one. First note that $b = 1$ means that the area under θ, see Figure 4, is

$$\theta(1) + \frac{1}{2}(\phi\bar{\theta} - \theta(1)). \tag{32}$$

Second, recall that the users' time in the unitary cycle time is an invariant, and thus we have

$$\theta(1) = \bar{\theta}(2 - \phi) \geq 0, \forall\phi \leq 2. \tag{33}$$

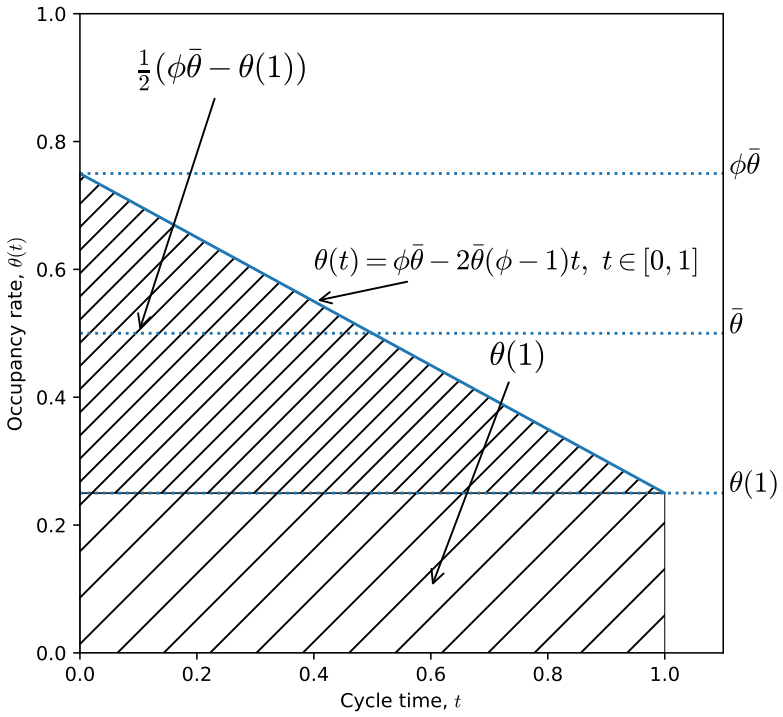

Fig. 6 Derivation of $\theta(1)$ for $\phi \leq 2$.

A value of ϕ larger than two may represent strongly unbalanced passenger flows in radial lines, even though this would imply that a fraction of the cycle time is represented by zero occupancy rate in the linear approximation.

Let a and A be the abscissa in the domain of $\theta(t)$ where this function is at its minimum distance from the θ_{min} level, and the area under $\theta(t)$ in the interval $[0, a]$, respectively.

The right-hand side of (30) is then

$$\begin{aligned}&\int_0^a \theta(t)(1+\rho(\theta(t)-\theta_{min}))\mathrm{d}t + \int_a^1 \theta(t)\mathrm{d}t\\ &= \int_0^1 \theta(t)\mathrm{d}t + \rho\left(\int_0^a \theta^2(t)\mathrm{d}t - \theta_{min}\int_0^a \theta(t)\mathrm{d}t\right)\\ &= \bar{\theta} + \rho\left(\int_0^a \theta^2(t)\mathrm{d}t - \theta_{min}A\right),\end{aligned}$$

and the function Δ_2 is

$$\Delta_2 = 1 + \rho\left(\frac{1}{\bar{\theta}}\int_0^a \theta^2(t)\mathrm{d}t - \theta_{min}\frac{A}{\bar{\theta}}\right). \tag{34}$$

Observe that whenever crowding does not occur, $\theta(0) = \phi\bar{\theta} \leq \theta_{min}$, a and A are both equal to zero, and (34) yields $\Delta_2 = 1$, as expected. Equation (34) holds for the other relevant cases that are dealt in the following. First, observe that $a < b$ for $\theta_{min} > 0$, and

$$\begin{aligned}\int_0^a \theta^2(t)\mathrm{d}t &= \int_0^a \left[(\phi\bar{\theta})^2 + c^2t^2 - 2c\phi\bar{\theta}t\right]\mathrm{d}t\\ &= (\phi\bar{\theta})^2 a + \frac{c^2a^3}{3} - c\phi\bar{\theta}a^2.\end{aligned}$$

In the case of $\phi \leq 2$ and $\bar{\theta}(2-\phi) < \theta_{min} < \phi\bar{\theta}$ (illustrated in Figure 4), by simple geometric analysis, we have:

$$\begin{aligned}a &= \frac{\phi\bar{\theta} - \theta_{min}}{2\bar{\theta}(\phi-1)}\\ c &= 2\bar{\theta}(\phi-1)\\ A &= \frac{a}{2}(\phi\bar{\theta} + \theta_{min}) = \frac{(\phi\bar{\theta})^2 - \theta_{min}^2}{4\bar{\theta}(\phi-1)}.\end{aligned}$$

In the case of $\phi \leq 2$ and $\theta_{min} \leq \bar{\theta}(2-\phi)$ (illustrated in Figure 8) we have:

$$\begin{aligned}a &= 1\\ c &= 2\bar{\theta}(\phi-1)\\ A &= \bar{\theta}.\end{aligned}$$

In the case of $\phi > 2$ and $\theta_{min} < \bar{\theta}\phi$ (illustrated in Figure 9) we have:

$$\begin{aligned}a &= \frac{2(\phi\bar{\theta} - \theta_{min})}{\phi^2\bar{\theta}}\\ c &= \frac{\phi^2\bar{\theta}}{2}\\ A &= \frac{a}{2}(\phi\bar{\theta} + \theta_{min}) = \frac{(\phi\bar{\theta})^2 - \theta_{min}^2}{\phi^2\bar{\theta}}.\end{aligned}$$

This analysis allows us to define the function Δ_2 reported in Table 4. Figure 10 illustrates the difference among the crowding penalty functions δ, Δ, and Δ_2.

Table 4 Formula of the approximation of the multi-segment crowding penalty.

$$\Delta_2(\bar{\theta}) = \begin{cases} 1 + \rho\left(\phi^2\dfrac{\phi\bar{\theta}-\theta_{min}}{2(\phi-1)} + \dfrac{(\phi\bar{\theta}-\theta_{min})^3}{6\bar{\theta}^2(\phi-1)} - \phi\dfrac{(\phi\bar{\theta}-\theta_{min})^2}{2\bar{\theta}(\phi-1)} - \theta_{min}\dfrac{(\phi\bar{\theta})^2-\theta_{min}^2}{4\bar{\theta}^2(\phi-1)}\right) & \bar{\theta}(2-\phi) < \theta_{min} < \phi\bar{\theta}, \phi \leq 2 \\ 1 + \rho\left(\phi^2\bar{\theta} + \dfrac{4\bar{\theta}(\phi-1)^2}{3} - 2\phi\bar{\theta}(\phi-1) - \theta_{min}\right) & \theta_{min} \leq \bar{\theta}(2-\phi), \phi \leq 2 \\ 1 + \rho\left(2(\phi\bar{\theta}-\theta_{min}) + \dfrac{2(\phi\bar{\theta}-\theta_{min})^3}{3(\phi\bar{\theta})^2} - \dfrac{2(\phi\bar{\theta}-\theta_{min})^2}{\phi\bar{\theta}} - \theta_{min}\dfrac{(\phi\bar{\theta})^2-\theta_{min}^2}{(\phi\bar{\theta})^2}\right) & \theta_{min} < \phi\bar{\theta}, \phi > 2 \\ 1 & \theta_{min} \geq \phi\bar{\theta} \end{cases}.$$

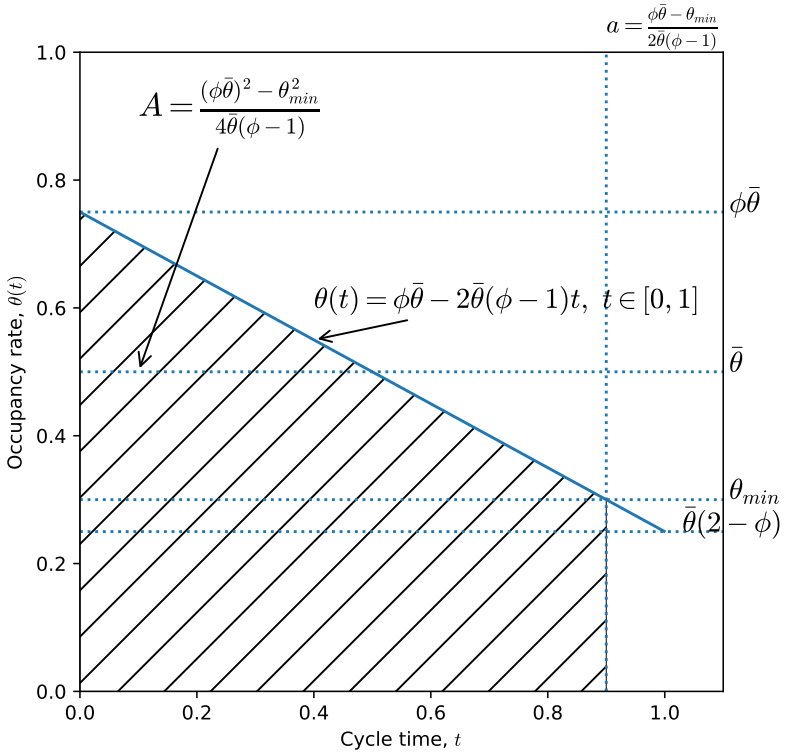

Fig. 7 Example of a linear occupancy rate function with $\phi \leq 2$ and $\bar{\theta}(2 - \phi) < \theta_{min} < \phi\bar{\theta}$.

5 Numerical experiments

This section is structured as follows. Section 5.1 describes the case study, its parameters, and the way in which we label the numerical experiments. The results of the spatially disaggregated and aggregated models are discussed in Section 5.2.

5.1 Parameters and experiment labeling

We present extensions of a scenario introduced in Moccia et al. (2018) and denoted there as "Scenario 2". This scenario represents an exclusive at grade right-of-way where traffic signal priority is provided. Stations are multi-modal transfer points and allow off-vehicle fare collection, level boarding, and other passenger amenities as detailed in Moccia et al. (2018). Rail TUs may operate as multiple units with a number of vehicles ranging from one to four. Buses are either single-articulated vehicles of 18 m in length, or double-articulated of 24 m in length. The maximum authorized speed is assumed to be the same for each of the three technologies (75 km/h).

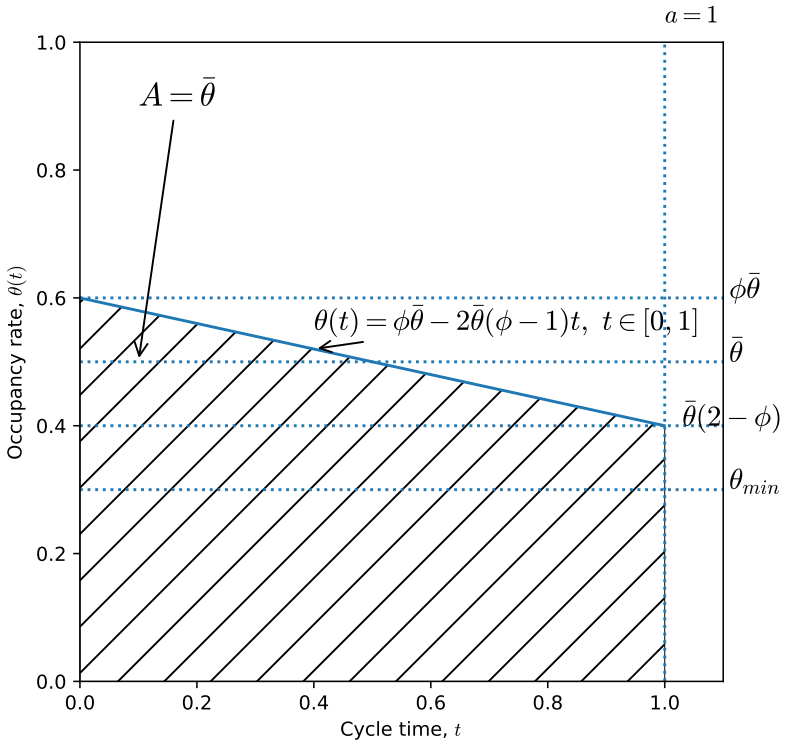

Fig. 8 Example of a linear occupancy rate function with $\phi \leq 2$ and $\theta_{min} \leq \bar{\theta}(2 - \phi)$.

We introduce labels to differentiate among the experiments as follows. A technology is indicated by three letters, "BRT" or "LRT", to distinguish between bus and rail, respectively, and, in the case of a single-unit technology, a number specifying the length of the vehicle in meters. For example, the label "BRT_18" refers to the BRT with an 18 m bus. The parameters related to the users and to the transit line that are common to all scenario variants are listed in Table 5. Table 6 lists the parameters that are mode-specific, and Table 7 reports those that are technology-specific. Monetary figures are expressed in US dollars for the year 2012. Capital amortization per hour of service is computed by formula (44) for infrastructure and rolling stock. Land capital cost is annualized by multiplying it by the discount rate, i.e. assuming an infinite service life. We consider four periods, and the period-related parameters are listed in Table 8. These parameters derive from the same temporal distribution of the demand used in Moccia et al. (2018), the difference being that we now discretize the service time by four periods instead of three as in the previous paper. This is because an even number of periods simplifies the construction of instances for the spatial attributes, as explained in the following.

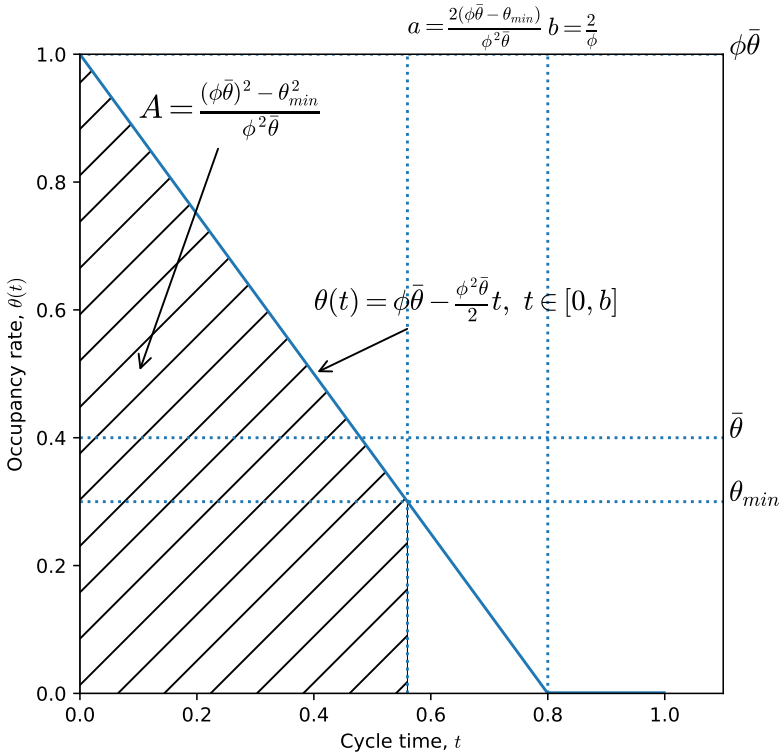

Fig. 9 Example of a linear occupancy rate function with $\phi > 2$ and $\theta_{min} < \bar{\theta}\phi$.

We introduce two scenario variants for the spatial variability of the demand. The first, denoted as "diametrical" and abbreviated by the letter "D", locates the main traffic attractor in a central sector of the line, and the second, denoted as "radial" and abbreviated by the letter "R', locates it at or near one end of the line. Thus, for example, "D_BRT_18" refers to the diametrical scenario variant for the BRT_18 technology, and "R_LRT" refers to the radial scenario variant for the LRT technology. There are four sectors, $m = 4$, and the sector lengths are the same for both scenario variants (Table 9). For each variant we use two spatially disaggregated profiles such that one can be obtained by a change of direction of the other. The first of these two profiles is assigned to the periods one and three, and the second is assigned to the periods two and four — and this is the reason why for simplicity we have discretized the service time into four periods. Figure 11 and 12 depict for the diametrical case the boarding and alighting parameters of the first and second profiles, respectively. For the radial case the first profile is that of Figure 4, which was used to introduce the notation, and the second is illustrated in Figure 13.

We apply two models to these two scenario variants, the spatially disaggregated model introduced in this paper, and the spatially aggregated model of Moccia et al.

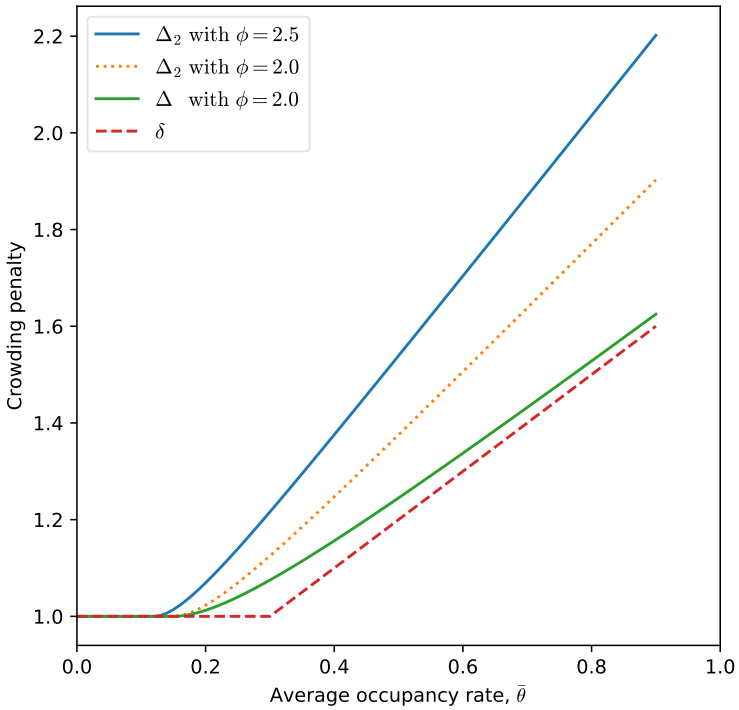

Fig. 10 Examples of the crowding penalty functions δ, Δ, and Δ_2 for the same values of $\rho = 1$ and $\theta_{min} = 0.3$.

(2018) with the new crowing penalty function introduced in Section 4 of this paper. In reporting results we label by the letters "M" and "S" those of the spatially disaggregated and aggregated models, respectively. For example, "R_M_BRT_24" refers to the spatially disaggregated model applied to the radial case for the technology "BRT_24". Whenever the model is not indicated we report results for both models, e.g. "R_BRT_24' refers to the results of both studied models.

The spatially aggregated model does not use the sector- and segment-specific parameters (Figures 4 and 11–13) and needs other parameters to synthetically represent the spatial distribution of the demand. These parameters are: α, the fraction of demand in the most loaded segment of the line; λ, the ratio of the average trip length to the length of the route; ϕ, the ratio of the maximum to the average occupancy rate; and ψ, the ratio of the maximum to the average dwell time. The first three of these parameters are uniquely determined by the spatially disaggregated data. Specifically, α is immediately readable from the spatially disaggregated profiles (Figures 4 and 11–13), and λ requires the following

precomputation:

$$\lambda = \sum_j \bar{\Upsilon}_j \Lambda_{e(j)}. \tag{35}$$

Figures 14 and 15 illustrate the linear approximation of the occupancy rate for the two scenario variants by the method presented in Section 4, and provide the values of ϕ. Note that these figures are constructed by the approximation of the cycle time to the cycle length, and under this assumption the following holds:

$$\phi = \frac{2\alpha}{\lambda}. \tag{36}$$

The last parameter, ψ, requires an iterative fine-tuning until a good accord between the results of the two models is reached in terms of the maximum dwell time. These four parameters of the spatially aggregated model are listed in Table 10 for the two scenario variants. The model is executed on 59 peak hour demand levels q uniformly spaced between 2000 and 60000 pax/h, extrema included.

Table 5 Parameters related to the users and to the transit system that are common to all scenario variants and all technologies.

Parameter	Symbol	Unit	Value
Unit operator cost per TU-hour	c_{1t}	$/TU-h	60
Upper bound of the stop spacing	d_{max}	km	2.5
Threshold frequency for timetable behavior	f_l	TU/h	6.0
Threshold frequency for the high frequency penalty	$\dot{f}$	TU/h	25
Number of service hours per year	H	h/year	5940
Route length	L	km	20.0
Land acquisition unitary cost	-	m$/hectare	10.7
Maximum allowed speed	S_{max}	km/h	75
Unit value of access time	V_a	$/h	20.05
Unit value of waiting time	V_w	$/h	16.71
Unit value of in-vehicle time	V_v	$/h	13.37
Waiting time at a stop when $f < f_l$	w	min	5
One-stage infrastructure technical life (route and stations)	y	year	40
Moltiplicative factor of the operating cycle time	β	-	1.07
Rate of the average waiting time to the headway	ϵ	-	0.5
Spare capacity factor for the fleet	ζ	-	1.20
Average occupancy rate up to $\delta = 1$	θ_{min}	-	0.3
Discount rate	ι	-	0.03
Discount factor of the waiting time under timetable behavior	μ	-	$0.\overline{3}$
Spare capacity factor for the TU	ν	-	0.95
Ratio of the residual value to the initial value of the rolling stock	Ξ	-	0.05
Ratio of the residual value to the initial value of the infrastructure	Ξ	-	0.00
Slope of the linear part of δ	ρ	-	1.0

Table 6 Mode-specific parameters.

Parameter	Symbol	Unit	BRT	LRT
Route width (two-ways)		m	10	9
One-stage vehicle technical life	y	year	12	25
Average acceleration rate	$\bar{a}$	m/s^2	1.00	1.15
Average deceleration rate	$\bar{b}$	m/s^2	1.15	1.00
Threshold frequency for platooning	f_m	TU/h	40	-
Cap on the maximum frequency	$\bar{f}_{max}$	TU/h	80	40
Parameter of the high frequency penalty	ω_1	-	0.075	0.135
Exponent of the high frequency penalty	ω_2	-	1.25	1.40

Table 7 Technology-specific parameters.

Parameter	Symbol	Unit	BRT_18	BRT_24	LRT
Route capital cost	-	m$/km	8.90	8.90	15.58
Route maintenance cost	-	m$/km-year	0.05	0.05	0.012
Stop capital cost, one-way	-	m$/stop	1.36	1.46	1.42
Stop maintenance cost, one-way	-	$/stop-year	37640	45276	35236
Incremental stop capital cost per additional vehicle, one-way	-	m$/stop-veh	0.00	0.00	0.73
Incremental stop maintenance cost per additional vehicle, one-way	-	$/stop-veh-year	0	0	24184
Vehicle capital cost	-	m$/veh	0.75	1.00	2.9
Vehicle capacity	k	pax/veh	114	154	191
Unit operator cost per vehicle-km	c_{2v}	$/veh-km	1.71	2.30	1.96
Vehicle administrative cost	c_{1vb}	$/veh-year	44230	45437	54908
Time lost at intersections per average km	t_u	min/km	0.74	0.74	0.62
Fixed time lost for a stop (doors and others fixed times)	t_d	s	6.0	7.0	7.0
Vehicle alighting time per user	t_{ba}	s-veh/pax	0.8	0.5	0.5
Vehicle boarding time per user	t_{bb}	s-veh/pax	1.3	0.9	0.9
Fixed terminal time	t_{tf}	s	360	360	210
Variable terminal time	t_{tv}	s	0	0	80
Minimum number of vehicles per transit unit	n_{min}	veh/TU	1	1	1
Maximum number of vehicles per transit unit	n_{max}	veh/TU	1	1	4
Fraction of the longest dwell time in the maximum frequency formula	η	-	0.571	0.571	1.000
Fixed stop clearance time	t_{e0}	s	32	34	57
Stop clearance time for an extra vehicle length	t_{ev}	s/veh	0	0	2

Table 8 Period-related parameters common to all scenario variants and all technologies.

Ratio	Symbol	$p = 1$	$p = 2$	$p = 3$	$p = 4$
Period average demand to average peak demand	γ_p	1.00000000	0.61421007	0.39064449	0.13704000
Maximum to average peak period demand	τ_p	1.27952633	1.35324947	1.21027921	2.40126798
Period hours to total service hours	χ_p	0.08009259	0.13043981	0.20509259	0.58402778

Table 9 Sector-related parameters common to all scenario variants and all technologies.

Ratio	Symbol	$i = 1$	$i = 2$	$i = 3$	$i = 4$
Fraction of the route length	Λ_i	0.35	0.25	0.20	0.20

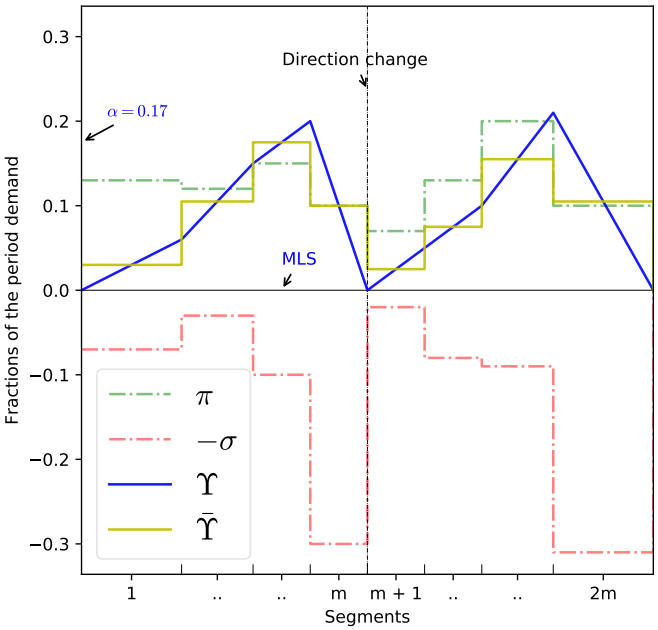

Fig. 11 Diametrical scenario variant, spatially disaggregated demand profile, periods one and three.

Table 10 Parameters for the spatially aggregated model.

Parameter	Symbol	Value for the diametrical case	Value for the radial case
Fraction of demand in the most loaded segment of the line	α	0.175	0.365
Ratio of the average trip length to the length of the route	λ	0.187	0.215
Ratio of the maximum to the average occupancy rate	ϕ	1.869	3.399
Ratio of the maximum to the average dwell time	ψ	1.550	2.100

5.2 Results

We now report results of the spatially disaggregated and aggregated models for the three technologies and two scenario variants presented in Section 5.1. Because the two scenario variants differ in the average journey length, we report results according to a passenger travel density (PTD) index which expresses the amount of traveled distance by passengers per unit of route length. This index is defined as

$$\text{PTD} = Hq\lambda \sum_{p} \chi_p \gamma_p, \tag{37}$$

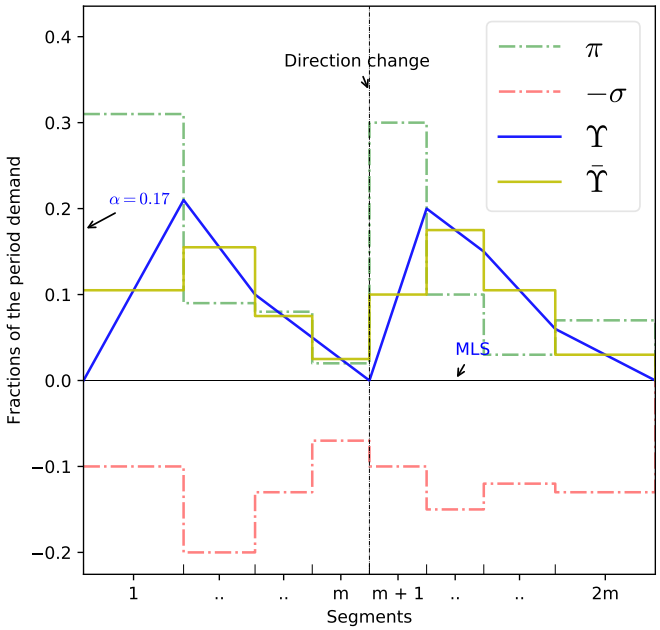

Fig. 12 Diametrical scenario variant, spatially disaggregated demand profile, periods two and four.

and its unit of measure is pax-km/year-km, where the "km" in the numerator refers to the unitary distance traveled by a passenger, and the "km" in the denominator expresses the unitary route length. The studied range of peak hour demands and the other parameters of the two scenario variants yield PTDs between $\sim 7 \times 10^5$ and $\sim 2 \times 10^7$ pax-km/year-km.

We first compare the total cost and its two components, user and operator costs, of the two models. We compute the percent absolute difference between these costs as $\mid C_1 - C_2 \mid /C_1 \times 100$, where the subscripts "1" and "2" indicate the disaggregated and aggregated models, respectively. Box and whisker plots of Figures 17–22 illustrate this comparison for the six technology-scenario combinations. These box and whisker plots use the following data visualization scheme. The box represents the interquartile range (IQR), i.e. it extends from the first to the third quartile values of the data. The band inside the box is the median. The whiskers represent the lowest datum still within 1.5 IQR of the first quartile, and the highest datum still within 1.5 IQR of the third quartile. The data outside the whiskers' range are the outliers and are indicated by circles. The average value is indicated by a triangle. In terms of total cost, the third quartile is very small, below 1% for all but one results' set, and also the outliers are small. In terms of user and operator costs, there are few significant outliers but the upper whisker remains below 4% for all results' sets. This allows us to conclude that the spatially aggregated model suffices with respect to a more involved and data-intensive

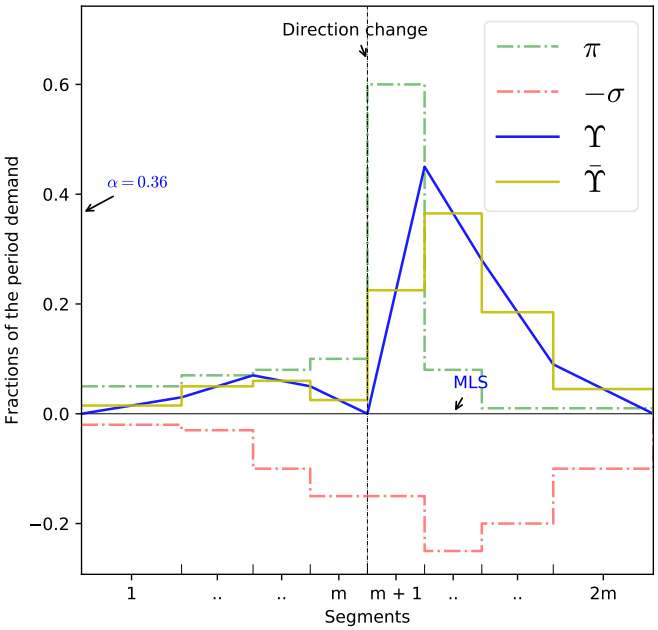

Fig. 13 Radial scenario variant, spatially disaggregated demand profile, periods two and four.

spatial disaggregation when the total cost is the metric of interest, as in the case of technology selection. This high accuracy of the spatially aggregated model is due to the new crowding penalty function introduced in Section 4. For brevity, and for the reasons explained in the following, we omit the results of the spatially aggregated model with the penalty function Δ of Moccia et al. (2018). First, observe that the previous crowding penalty function is defined for ϕ not larger than two, and therefore would not be appropriate to use for the radial case where ϕ is larger than two. Second, even limiting the comparison to the diametrical case, where ϕ is smaller than two, the previous penalty function would have yielded percent absolute differences between the total costs of the two models larger than the double of what previously reported. These results are available upon request from the corresponding author. Figures 23 and 24 illustrate the average crowding penalty under the diametrical scenario variant for the spatially disaggregated and aggregated models, respectively. These figures allow us to conclude that an excellent agreement exists between these two models for the average crowding penalty under the diametrical scenario variant. Figures 25 and 26 allow us to reach the same conclusion for the radial case.

Figures 27–32 depicts the stop spacings of the six technology and scenario variant combinations yielded by the spatially disaggregated model. The average stop spacings obtained by the spatially aggregated model are in good accord with those of the spatially disaggregated model, and therefore these figures are omitted

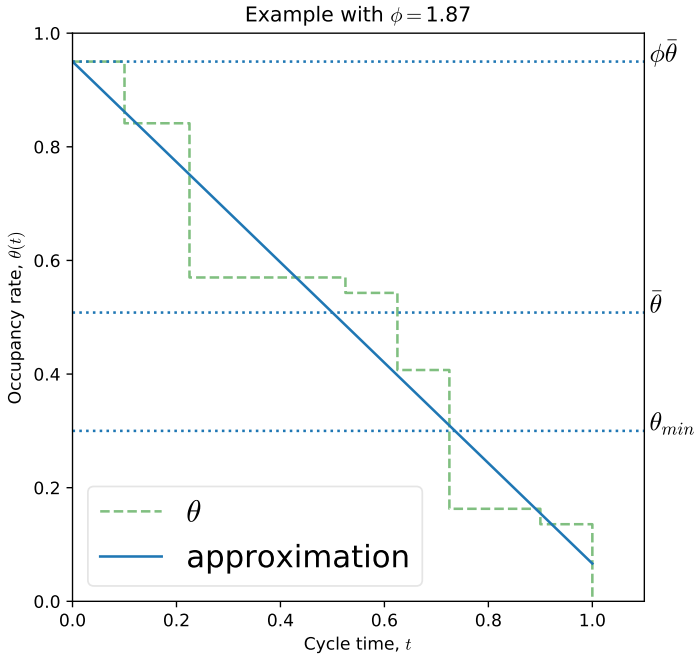

Fig. 14 Diametrical scenario variant, an example of occupancy rates in decreasing order and the linear approximation for the spatially aggregated model.

for the sake of brevity. As expected, the range of sector-specific stop spacings is larger under the radial than under the diametrical scenario variant. However, also under the diametrical case the differences between the sector-specific stop spacings and the average is of importance. This allow us to conclude that spatial disaggregation significantly increases accuracy when the main focus is line design instead of technology selection.

We now show the usefulness of the spatially disaggregated model for benchmarking. Vehicle occupancy is a key index to assess the under- or the over-utilization of a transit line. It is intuitive that this index should depend on vehicle capacity, passenger travel density, and spatial characteristics of the demand. Our model allows this type of analysis. Figures 33 and 34 illustrate the average vehicle occupancy (AVO) per unitary vehicle length of the three studied technologies under the diametrical and radial scenario variants, respectively. The radial case shows lower AVOs for a given PTD than the diametrical case, as may be expected from a system offering the improved connectivity of trips across the densest parts of the city. Figure 16, representing Edmonton's LRT system in 2008 when it had a basic diametrical configuration, exemplifies how symmetry of the passenger load profiles can appear in such a case.

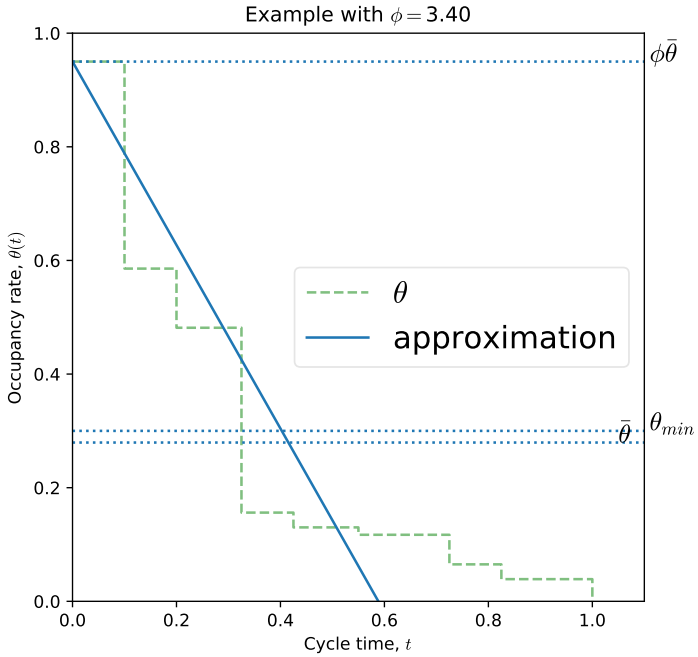

Fig. 15 Radial scenario variant, an example of occupancy rates in decreasing order and the linear approximation for the spatially aggregated model.

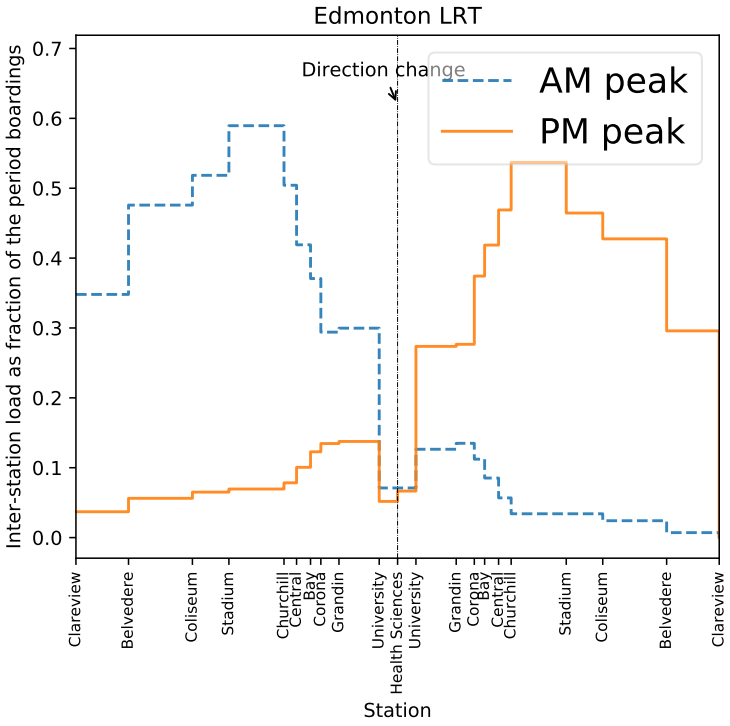

Fig. 16 AM and PM peak profiles in the Edmonton LRT, year 2008. Source: our elaboration from The City of Edmonton (2008).

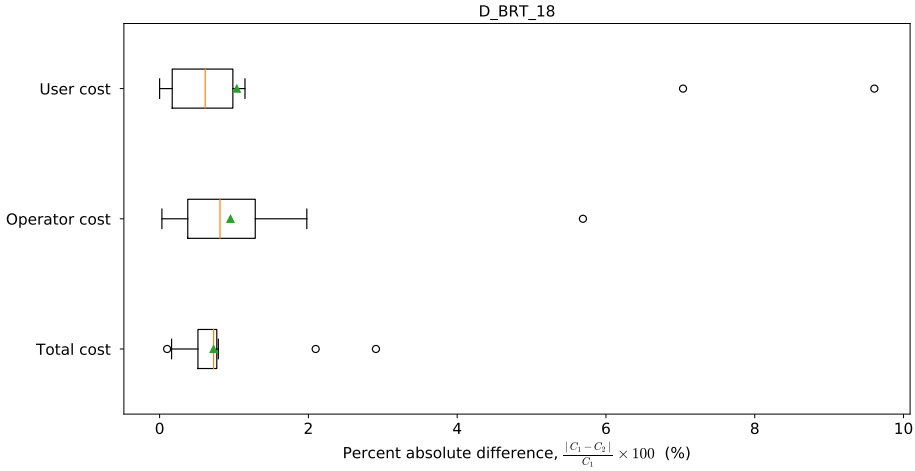

Fig. 17 Diametrical scenario variant and the BRT_18 technology: box and whisker plot of the percent absolute difference of the objective function and its two components of the two studied models.

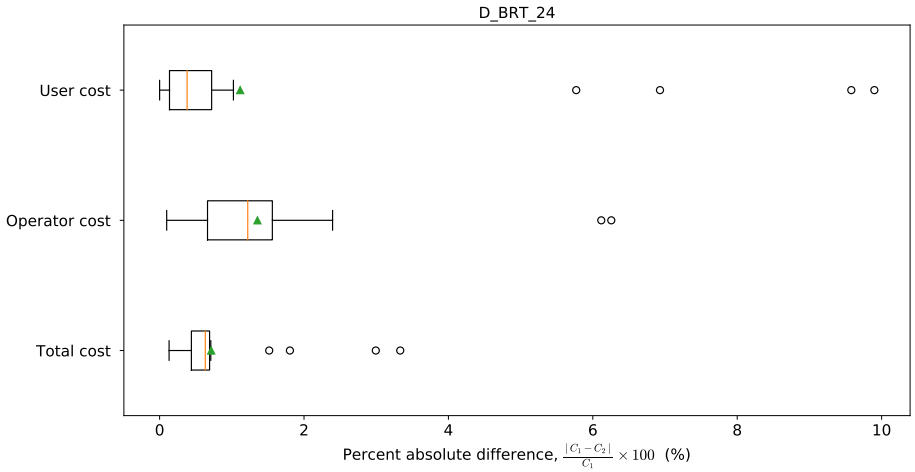

Fig. 18 Diametrical scenario variant and the BRT_24 technology: box and whisker plot of the percent absolute difference of the objective function and its two components of the two studied models.

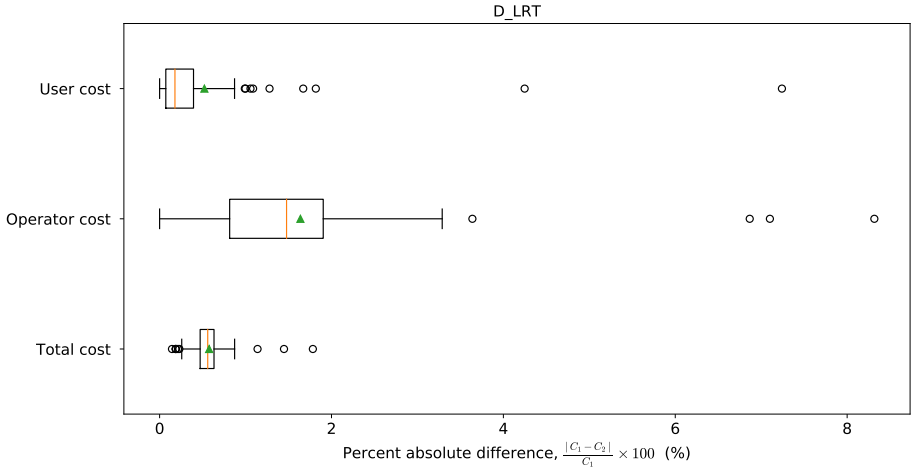

Fig. 19 Diametrical scenario variant and the LRT technology: box and whisker plot of the percent absolute difference of the objective function and its two components of the two studied models.

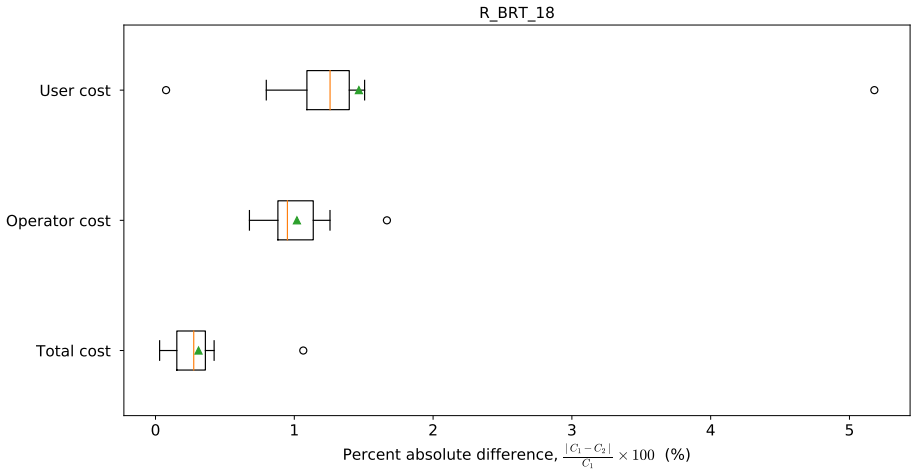

Fig. 20 Radial scenario variant and the BRT_18 technology: box and whisker plot of the percent absolute difference of the objective function and its two components of the two studied models.

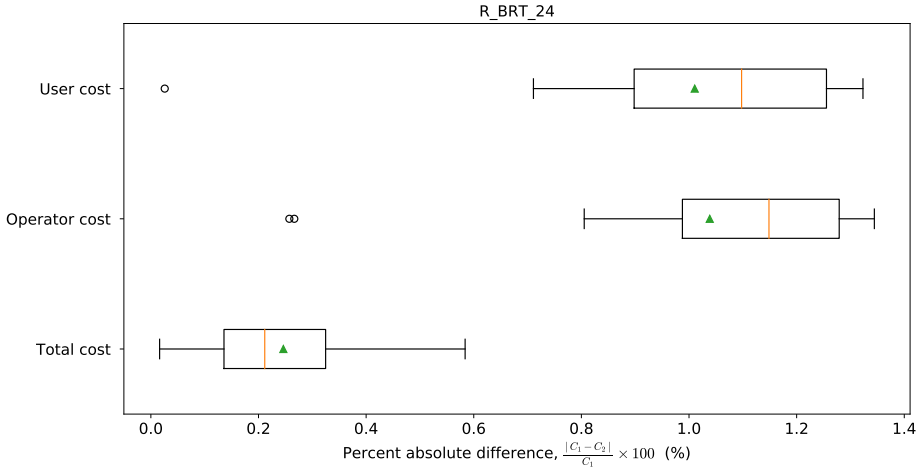

Fig. 21 Radial scenario variant and the BRT_24 technology: box and whisker plot of the percent absolute difference of the objective function and its two components of the two studied models.

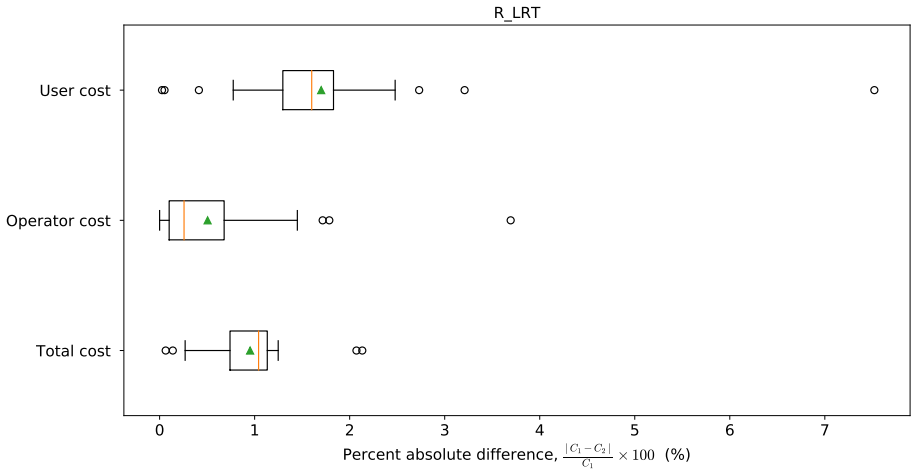

Fig. 22 Radial scenario variant and the LRT technology: box and whisker plot of the percent absolute difference of the objective function and its two components of the two studied models.

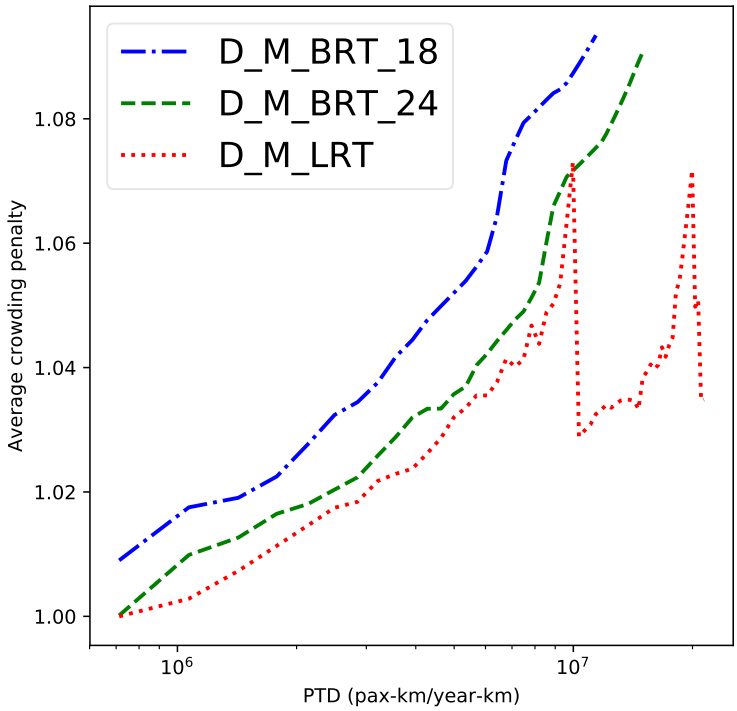

Fig. 23 Diametrical scenario variant and spatially disaggregated model: average crowding penalty of the three studied technologies by passenger travel density in logarithmic scale.

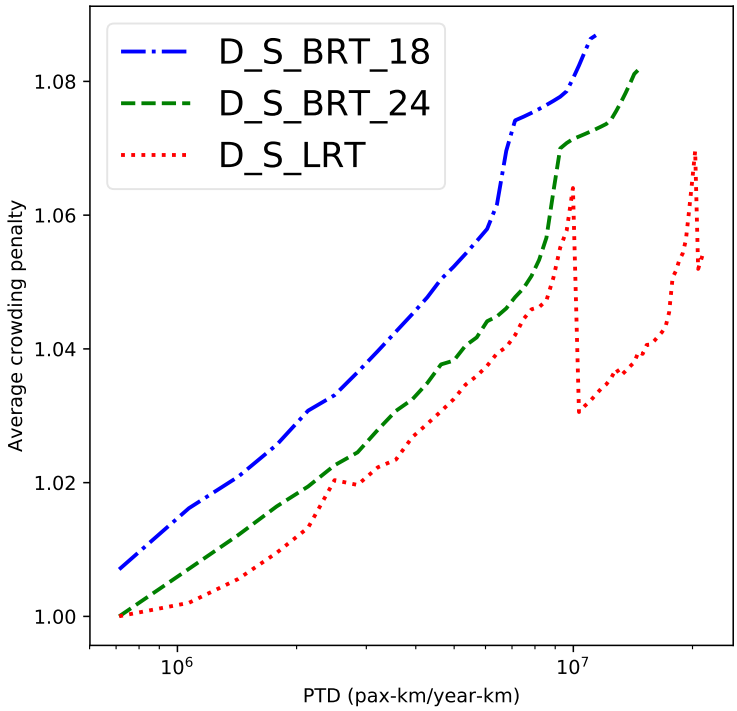

Fig. 24 Diametrical scenario variant and spatially aggregated model: average crowding penalty of the three studied technologies by passenger travel density in logarithmic scale.

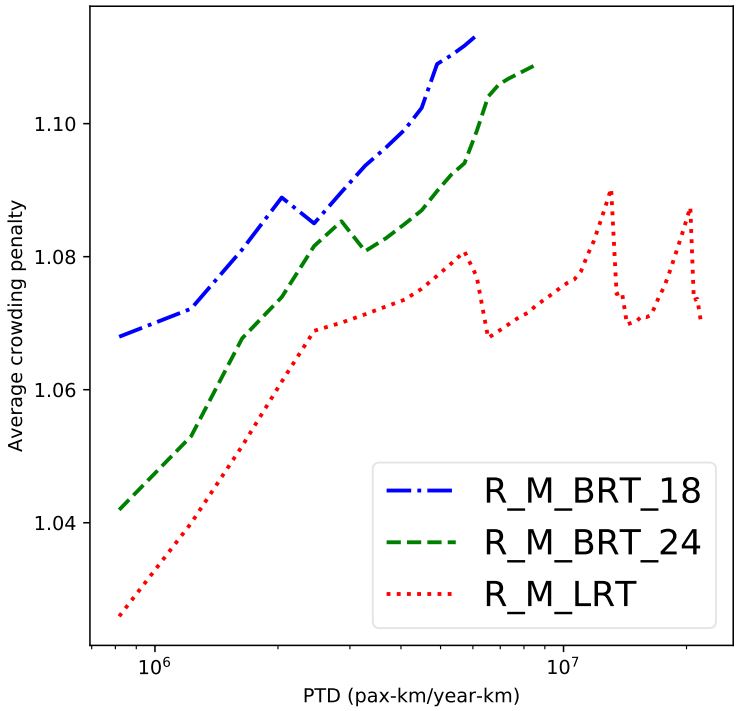

Fig. 25 Radial scenario variant and spatially disaggregated model: average crowding penalty of the three studied technologies by passenger travel density in logarithmic scale.

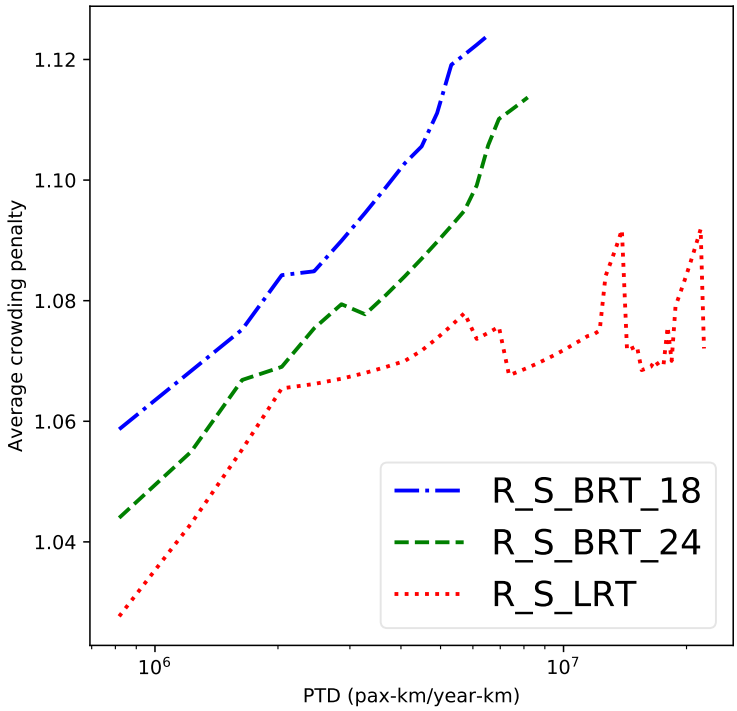

Fig. 26 Radial scenario variant and spatially aggregated model: average crowding penalty of the three studied technologies by passenger travel density in logarithmic scale.

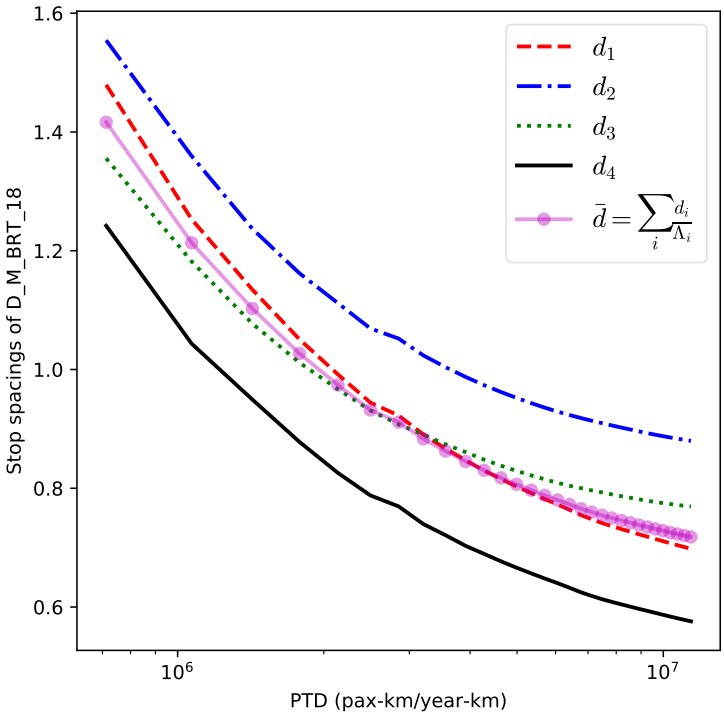

Fig. 27 Diametrical scenario variant, spatially disaggregated model and technology BRT_18: average stop spacing and sector-specific stop spacings by passenger travel density in logarithmic scale.

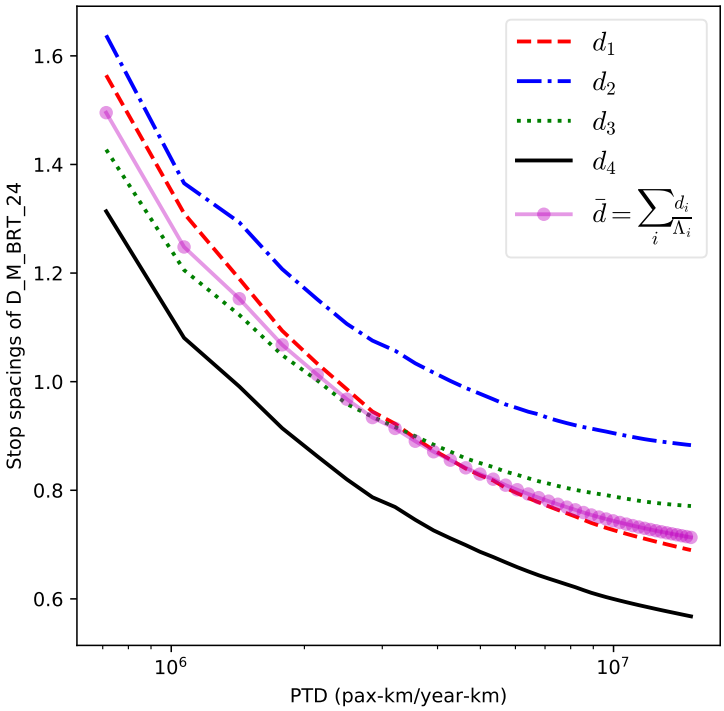

Fig. 28 Diametrical scenario variant, spatially disaggregated model and technology BRT_24: average stop spacing and sector-specific stop spacings by passenger travel density in logarithmic scale.

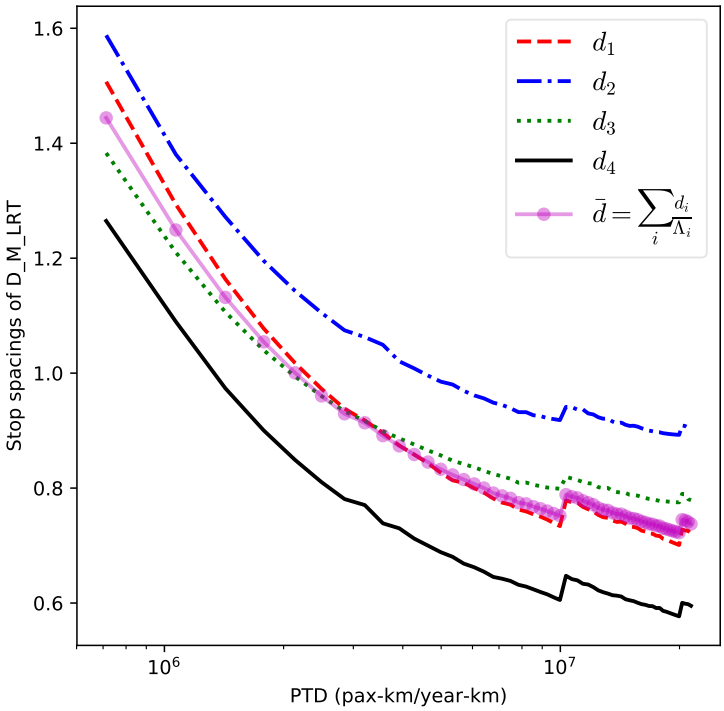

Fig. 29 Diametrical scenario variant, spatially disaggregated model and technology LRT: average stop spacing and sector-specific stop spacings by passenger travel density in logarithmic scale.

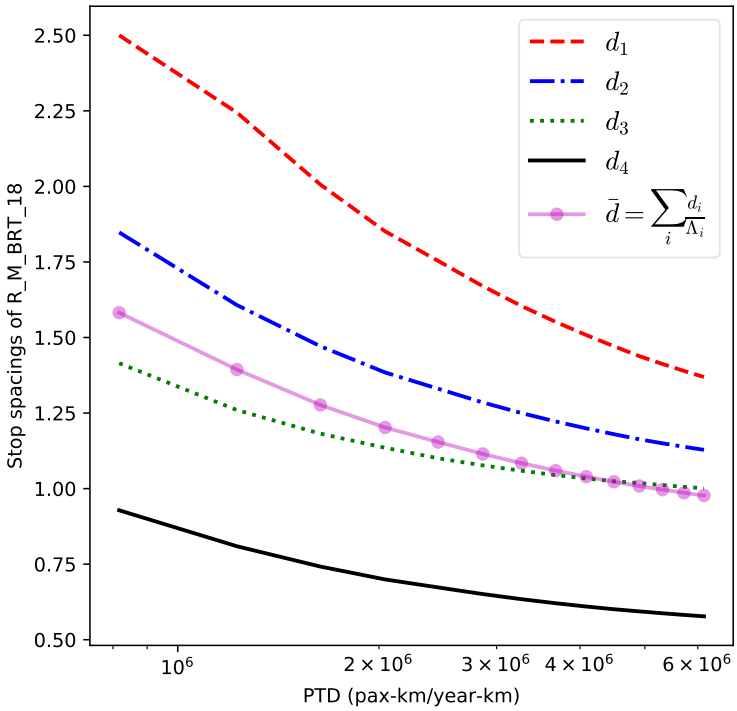

Fig. 30 Radial scenario variant, spatially disaggregated model and technology BRT_18: average stop spacing and sector-specific stop spacings by passenger travel density in logarithmic scale.

6 Conclusions

We have presented an optimization model for the technology selection and design of a transit line where the demand is spatially disaggregated by segments. In spite of some notational complexity, the model was solved by a method based on approximation formulae, as in the case of spatially aggregated demand. The approximation formula for stop spacing shares similarities with that of Wirasinghe and Ghoneim (1981) derived by a different method. The comparison between the spatially disaggregated and aggregated models has led us to devise a refinement of the crowding penalty function of the spatially aggregated model. We have presented numerical experiments that point to three main conclusions. First, the revised spatially aggregated model suffices when the main focus is technology selection. Second, the spatially disaggregated model show its usefulness for design purposes, because the average stop spacing may be not always representative. Third, the spatially disaggregated model may be used for benchmarking on transit performance

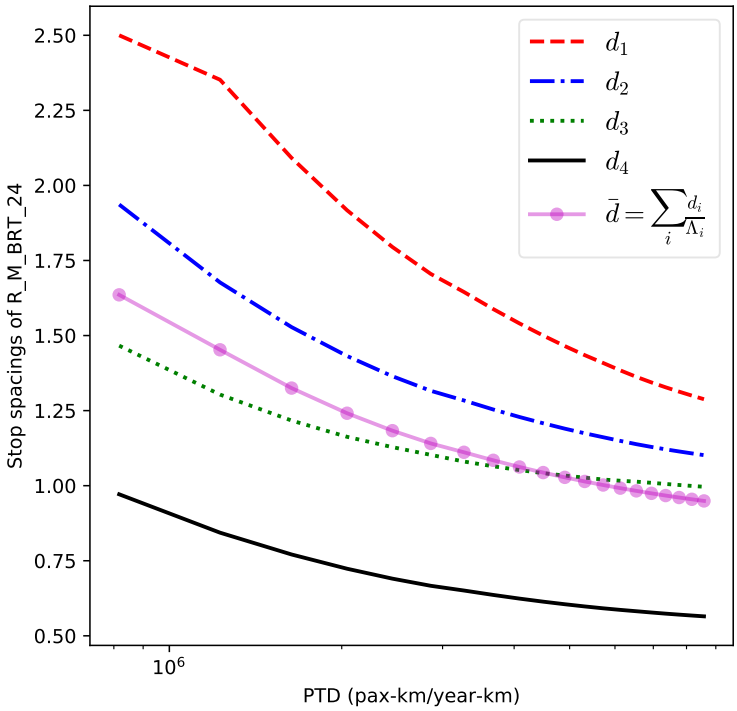

Fig. 31 Radial scenario variant, spatially disaggregated model and technology BRT_24: average stop spacing and sector-specific stop spacings by passenger travel density in logarithmic scale.

indices such as the average vehicle occupancy, which are strongly influenced by the type of spatial demand profile.

Acknowledgements

Luigi Moccia was partly supported by CNR (Italy) under project "Smart data and models". Gilbert Laporte was funded by the Canadian Natural Sciences and Engineering Research Council under grant 2015-06189. These supports are gratefully acknowledged. Luigi Moccia and Duncan W. Allen thank Eric C. Bruun for fruitful discussions on transit planning and operations. We thank the Editor and the referees for their valuable comments.

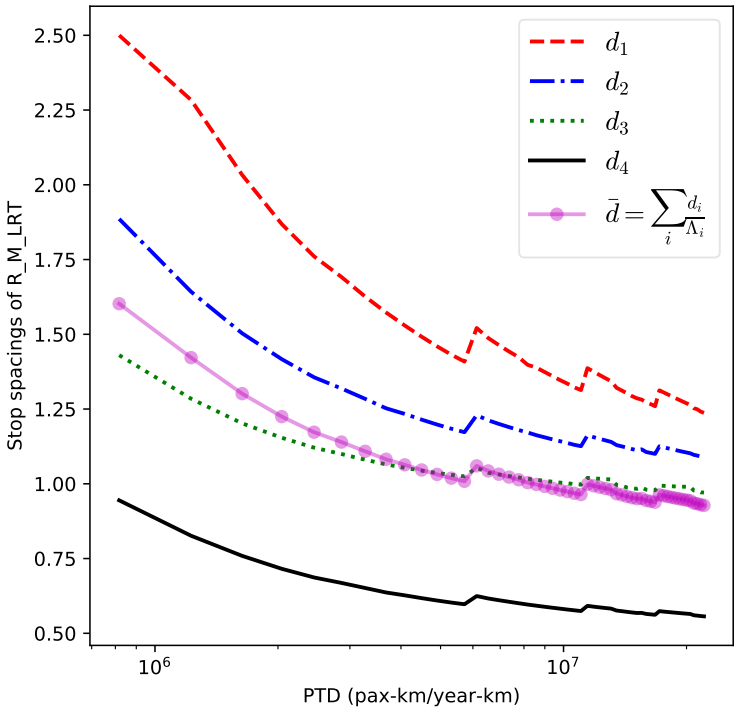

Fig. 32 Radial scenario variant, spatially disaggregated model and technology LRT: average stop spacing and sector-specific stop spacings by passenger travel density in logarithmic scale.

Appendix A — Formulae shared by the spatially disaggregated and aggregated models

Here we report formulae that are common to the spatially disaggregated model presented in this paper and in the spatially aggregated model of Moccia et al. (2018).

The average speed excluding user service at stops, S_{run}, is

$$S_{run} = \frac{1}{\frac{1}{S_{max}} + \frac{t_u}{60}} \quad S_{max}[\text{km/h}], t_u[\text{min/km}]. \tag{38}$$

Let $\bar{a}$ and $\bar{b}$ be the average acceleration and deceleration rates of a TU. The incremental time loss caused by the acceleration and deceleration phases is denoted by T_a, and is equal to

$$T_a = \frac{S_{run}}{25920}\left(\frac{1}{\bar{a}} + \frac{1}{\bar{b}}\right) \quad S_{run}[\text{km/h}], \bar{a}, \bar{b}[\text{m/s}^2], \tag{39}$$

(see e.g. Vuchic and Newell, 1968).

The lost time for acceleration, deceleration, and door opening and closing, T_l, is

$$T_l = T_a + \frac{t_d}{3600} \quad T_a[\text{h}], t_d[\text{s}]. \tag{40}$$

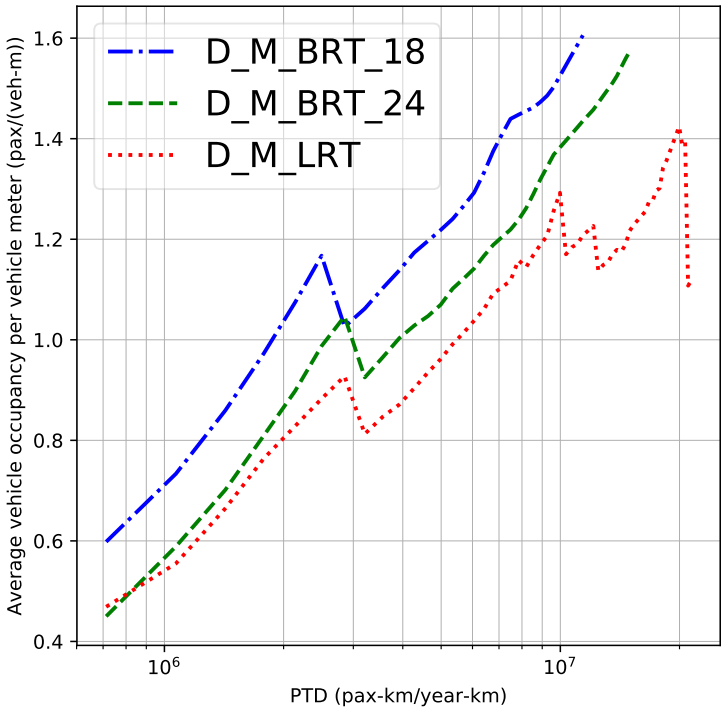

Fig. 33 Diametrical scenario variant and spatially disaggregated model: average vehicle occupancy per unitary vehicle length of the three studied technologies by passenger travel density in logarithmic scale.

The average waiting time t_w of a user is

$$t_w(f) = \begin{cases} \frac{w}{60} + \mu\frac{\epsilon}{f} & \text{if } f < f_l \\ \frac{\epsilon}{f} & \text{if } f_l \leq f \leq f_m, \\ \frac{\epsilon}{f_m} & \text{if } f > f_m \end{cases} \quad . \quad f[\text{TU/h}], w[\text{min}] \tag{41}$$

The lower bound for the frequency, f_{min}, is

$$f_{min} = \max\left\{f_{pol}, \frac{\alpha q \tau}{\nu k n}\right\} \; f_{pol}[\text{TU/h}], q[\text{pax/h}], k[\text{pax/veh}], n[\text{veh/TU}]. \tag{42}$$

The threshold value of the stop spacing, d_{min}, depends on acceleration and deceleration rates as follows

$$d_{min} = \frac{S_{max}^2}{25920}\left(\frac{1}{\bar{a}} + \frac{1}{\bar{b}}\right) \quad S_{max}[\text{km/h}], \bar{a}, \bar{b}[\text{m/s}^2], \tag{43}$$

(see e.g. Vuchic and Newell, 1968).

The capital amortization per hour of service is computed as

$$\frac{P(1-\Xi)\iota}{H(1-(1+\iota)^{-y})}, \tag{44}$$

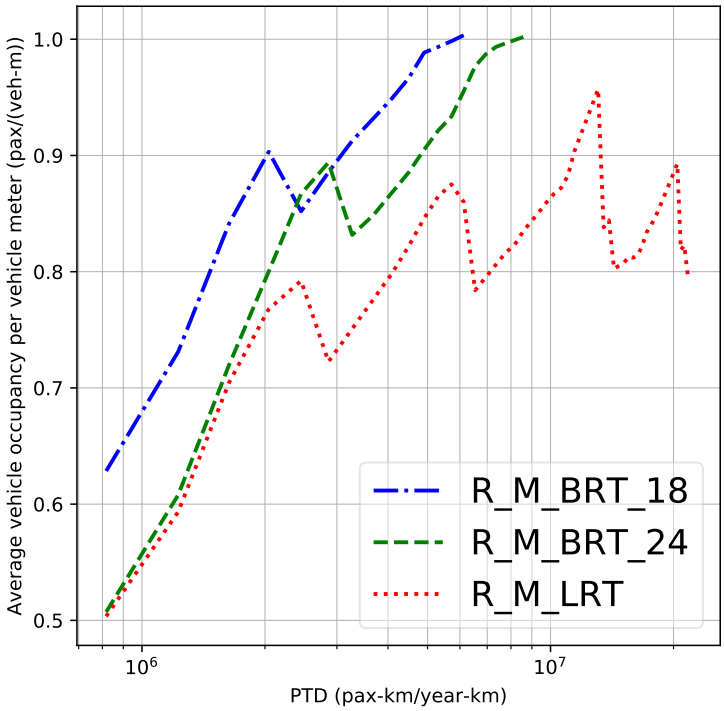

Fig. 34 Radial scenario variant and spatially disaggregated model: average vehicle occupancy per unitary vehicle length of the three studied technologies by passenger travel density in logarithmic scale.

where P is the purchase price, H is the number of service hours in a year, ι is the discount rate, Ξ is the fraction of the residual value, and y is the one-stage technical life. The one-stage technical life is lower than a typical service lifetime because it expresses the equivalent years including the cost of a mid-life rebuild at the prevalent discount rate.

References

Bruun, E. C., Allen, D. W., and Givoni, M. (2018). Choosing the right public transport solution based on performance of components. *Transport*, 33(4):1017–1029.

Byrne, B. F. (1975). Public transportation line positions and headways for minimum user and system cost in a radial case. *Transportation Research*, 9(2):97–102

City of Edmonton (2008). LRT ridership and park'n'ride report.

Daganzo, C. F. (2012). On the design of public infrastructure systems with elastic demand. *Transportation Research Part B: Methodological*, 46(9):1288–1293.

Daganzo, C. F., Gayah, V. V., and Gonzales, E. J. (2012). The potential of parsimonious models for understanding large scale transportation systems and answering big picture questions. *EURO Journal on Transportation and Logistics*, 1(1):47–65.

Gutiérrez-Jarpa, G., Laporte, G., Marianov, V., and Moccia, L. (2017). Multi-objective rapid transit network design with modal competition: The case of Concepción, Chile. *Computers & Operations Research*, 78:27–43.

Jara-Díaz, S. and Gschwender, A. (2003). Towards a general microeconomic model for the operation of public transport. *Transport Reviews*, 23(4):453–469.

Jensen, J. L. W. V. (1906). Sur les fonctions convexes et les inégalités entre les valeurs moyennes. *Acta Mathematica*, 30:175–193.

Laporte, G., Mesa, J. A., and Ortega, F. A. (1994). Assessing topological configurations for rapid transit networks. *Studies in Locational Analysis*, 7:105–121.

Laporte, G., Mesa, J. A., and Ortega, F. A. (1997). Assessing the efficiency of rapid transit configurations. *Top*, 5(1):95–104.

Moccia, L., Allen, D. W., and Bruun, E. C. (2016). New results of a technology choice model for a transit corridor. In *European Transport Conference 2016*. Association for European Transport (AET).

Moccia, L., Allen, D. W., and Bruun, E. C. (2018). A technology selection and design model of a semi-rapid transit line. *Public Transport*, 10:455–497.

Moccia, L., Giallombardo, G., and Laporte, G. (2017). Models for technology choice in a transit corridor with elastic demand. *Transportation Research Part B: Methodological*, 104:733–756.

Moccia, L. and Laporte, G. (2016). Improved models for technology choice in a transit corridor with fixed demand. *Transportation Research Part B: Methodological*, 83:245–270.

Newell, G. F. (1979). Some issues relating to the optimal design of bus routes. *Transportation Science*, 13(1):20–35.

TCQSM (2013). *Transit Capacity and Quality of Service Manual*. Transportation Research Board, Washington.

Tirachini, A., Hensher, D. A., and Jara-Díaz, S. R. (2010). Restating modal investment priority with an improved model for public transport analysis. *Transportation Research Part E: Logistics and Transportation Review*, 46(6):1148–1168.

Vuchic, V. R. (2005). *Urban Transit: Operations, Planning, and Economics*. Wiley, Hoboken.

Vuchic, V. R. and Newell, G. F. (1968). Rapid transit interstation spacings for minimum travel time. *Transportation Science*, 2(4):303–339.

Vuchic, V. R., Stanger, R. M., and Bruun, E. C. (2012). Bus rapid transit (BRT) versus light rail transit (LRT): Service quality, economic, environmental and planning aspects. In *Transportation Technologies for Sustainability*, pages 256–291. Springer, Berlin.

Wirasinghe, S. C. and Ghoneim, N. S. (1981). Spacing of bus-stops for many to many travel demand. *Transportation Science*, 15(3):210–221.